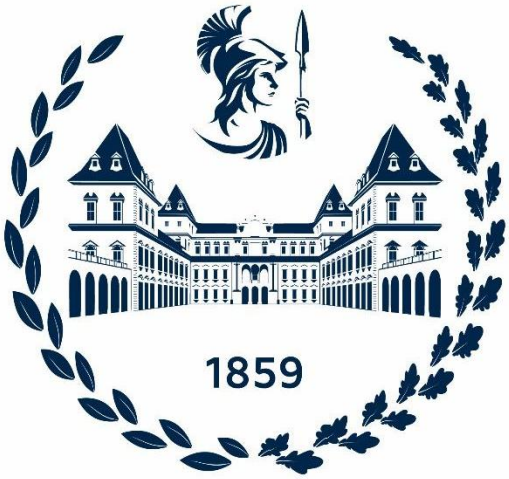

Politecnico di Torino

Master of Science in
Energy and Nuclear Engineering

Master of Science Thesis

Academic year 2021/2022

Design of a receiver for solar parabolic dish and Life Cycle Assessment of domestic hot water production system

Supervisior
Davide Papurello

Candidate
Ibrahim Tursunović

July 2022

Abstract

To limit global mean temperature to 1.5°C relative to pre-industrial levels, global CO_2 emissions must be decreased and become net zero at some point. As the energy sector is the main source of greenhouse gases, it also has the highest potential for improvement. [1] Improvements that can be reached by shifting to renewable energy sources. Concentrated solar plants coupled with thermal energy storage are a promising technology for dispatchable renewable energy. This technology can assure energy supply even in remote areas without contributing to greenhouse gases emissions during its operation. However, greenhouse gases, and other emissions, could be present during the fabrication process of components that make up the concentrated solar plant. For this reason, this thesis is composed of two main parts.

In the first part of master thesis is described the receiver design for thermal energy production of existing parabolic solar dish CSP plant, located at Energy Center of Politecnico di Torino. After theoretical introduction and literature review, by using COMSOL Multiphysics software, a receiver design will be proposed. The configuration will be analysed by using the Ray Tracing Module from the COMSOL library. The whole system in which parabolic dish operates is meant to be used for domestic hot water production in a residential family home.

In the second part of the thesis, Life Cycle Assessment analysis will be performed on the main components of the whole system used for domestic hot water production. The proposed configuration does not include any fossil back – up heat source so, during the operation phase of the system polluting emissions are absent. For this reason, the Life Cycle Assessment hereby presented, is focalised on the entire life cycle of main components: from cradle to grave. The main component included in the analysis are: solar collector, solar receiver, domestic hot water tank and piping system.

Abbreviations

Abbreviation	*Significate*
RES	*Renewable Energy Sources*
GHG	*Greenhouse Gases*
CSP	*Concentrated Solar Plants*
PCM	*Phase Change Materials*
SDS	*Sustainable Development Scenario*
SDH	*Solar District Heating*
DNI	*Direct Normal Irradiation*
HTF	*Heat Transfer Fluid*
LFR	*Linear Fresnel Reflector*
DHW	*Domestic Hot Water*
LCA	*Life Cycle Assessment*
FU	*Functional Unit*
CTUe	*Comparative Toxic Unit for ecosystems*
CTUh	*Comparative Toxic Unit for humans*

Contents

List of Tables

List of Figures

1 Introduction

The European green deal has the objective to make Europe the first continent in the World to be climate neutral by 2050 and to reduce GHG emissions at least by 55% before 2030. To reach these ambitious and unavoidable goals, the energy system of the whole continent must be transformed. As the energy sector accounts for more than 75% of EU's GHG emissions its decarbonization is needed to reach imposed targets [2]. The substitution of fossil fuels for the use of renewable energies does not pursue any other purpose than to implement sustainable development worldwide. With this, it is possible to break the trend of associating the economic development of a country and its energy consumption with the increase of greenhouse gas emissions.

Energy use for space and water heating has remained stable since 2010, with heating energy intensity decreasing by 2% per year since 2010 – insufficient to offset floor area growth. The heating equipment market is dominated by fossil fuel and less efficient conventional heating technologies. However, sales of renewable heating systems represent more than 10% of overall sales in 2019. To reach the Sustainable Development Scenario (SDS) goals, the share of clean energy technologies needs to exceed 50% of new heating equipment sales by 2030 [3]. In 2016, in EU countries, heating and hot water alone account for 79% of total final energy use [4]. Solar energy is a very adaptable renewable energy source and can be used to help reach the imposed goals.

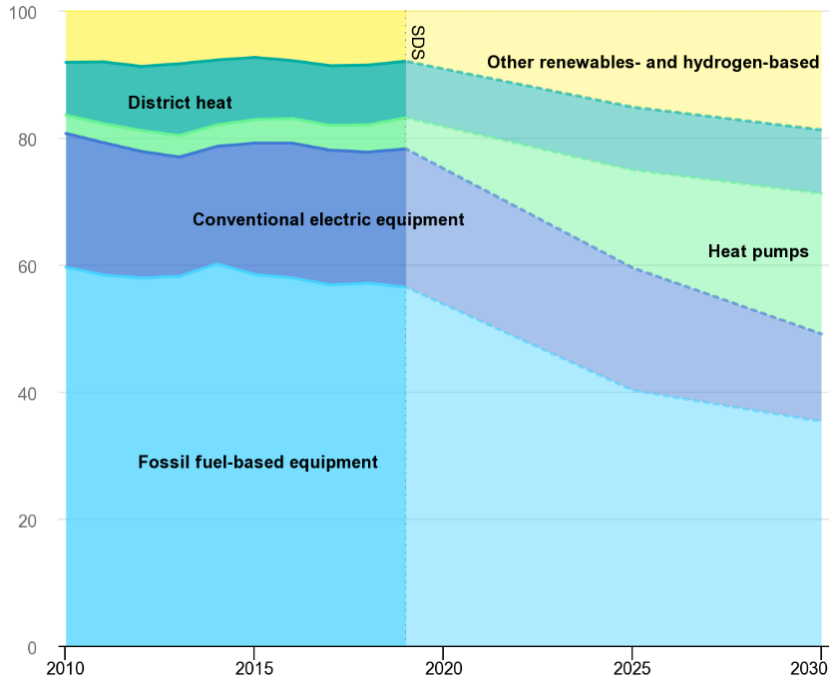

Figure 1 - Heating technologies sales in SDS. [3]

In this context CSP can play an important role. Nowadays most solar heat systems are related to low temperature heat demand in buildings, providing hot water and space heating. The solar heat can be used for individual houses and for district heating networks. As heating cannot be effectively traded, sold, or transported over long distances or across countries,

centralized solutions are preferred. To decarbonize the heating sector, mixing different technologies and solutions will be necessary, as the sector is huge. [5]

Solar energy is used across Europe in SDH projects that are at early market development stage. SDH is the field of solar thermal collectors supplying solar energy to the district heating network of a neighbourhood or a town. Solar collectors are supplemented by a central heating unit, which provides additional heat to meet the customer's demand. In most cases solar energy contributes up to 20% to annual heat demand. Using seasonal storage this can increase up to 60% or more. [6]

Concentrated solar power technologies receive more attention because of their high thermal efficiency for high and medium temperature range. Even if several CSP technologies are available, the parabolic dish system has the highest solar to thermal conversion efficiency with highest concentration ratio and can be employed for high temperature applications. [7] For efficient energy conversion, solar parabolic dish collectors can be equipped with a sun tracking system. The cavity receivers are preferred in solar to heat energy conversion due to low nominal heat losses. [8]

The work hereby presented aims at studying parabolic dish system receiver and its optimization starting from an initial configuration currently available at the Energy Center rooftop. The goal is to study the best receiver for production of domestic hot water in a residential sector. Particular attention must be devoted to receiver geometry and construction materials. Parabolic dish equipped with a proposed receiver will be able to meet energy demand for domestic hot water production for an residential building.

2 Theoretical framework

2.1 Solar Energy Overview

The Sun is the star at the center of the Solar System. Heated by nuclear fusion reactions, while fusing hydrogen to create helium, radiates the energy mainly as visible light, ultraviolet light, and infrared radiation.

Radiation emitted from the Sun has an energy distribution like that of a black body at a temperature of 6000 K. This radiation travels at $3 \cdot 10^8 \frac{m}{s}$ taking around 8 minutes to reach the Earth's atmosphere. The power received on a unit area of surface perpendicular to the direction of propagation of the radiation at mean earth – sun distance outside the atmosphere is called Solar Constant (G_{sc}) and has s value of 1377 $\frac{W}{m^2}$. [9]

Figure 2 represents the comparison between current annual energy consumption of the world, the known reserves of finite fossil and nuclear resources and the yearly potential of the renewable alternatives.

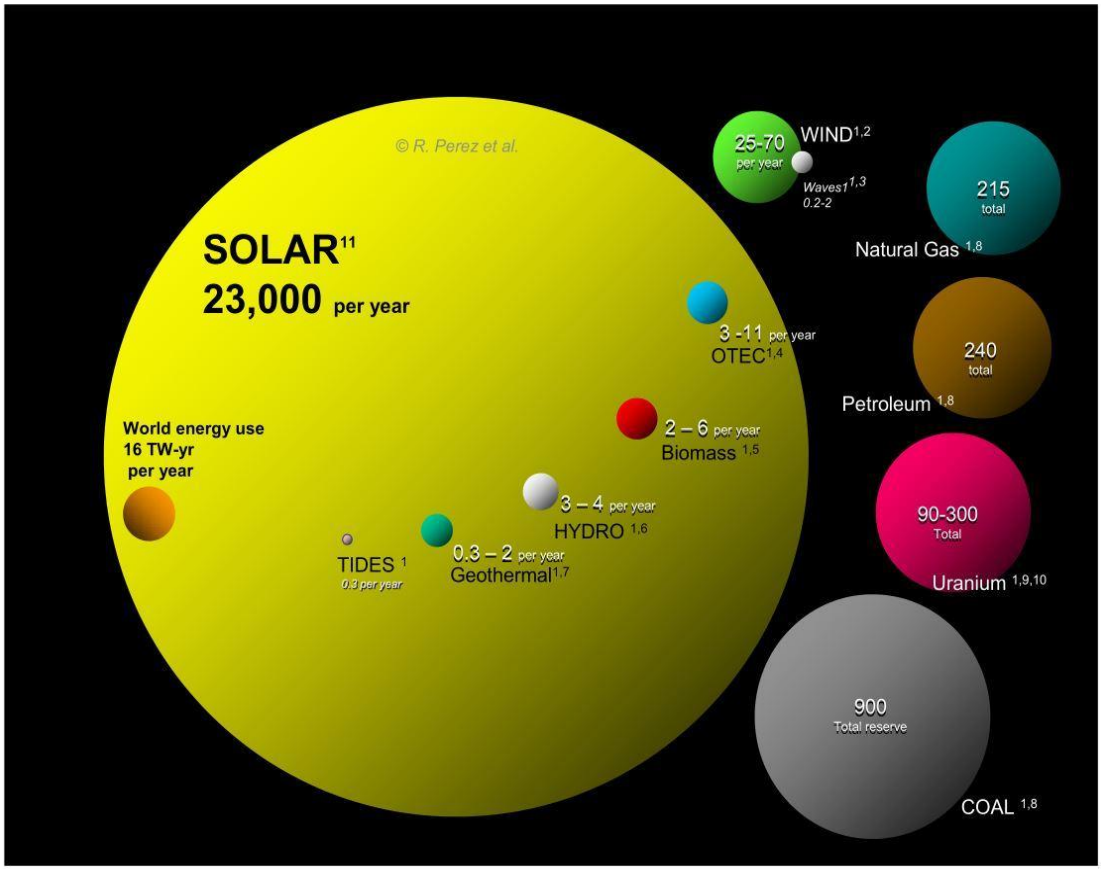

Figure 2 - Comparison between finite and renewable planetary energy reserves (Terawatt-years). Total recoverable reserves are shown for finite resources. Yearly potential is shown for renewables. [9]

Energy coming from the Sun every year is 1500 times larger than the total world energy use, as shown in Figure 2. However, as shown in the following Figure 4, only 2.6% of world gross electricity production has solar as primary energy. [10]

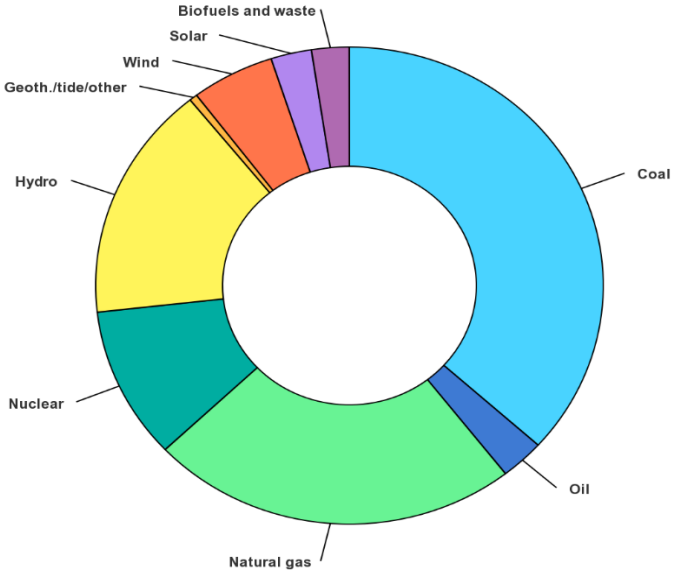

Even if the potential is massive (not only for solar but also for other renewable energy sources) in 2019 coal was still the main source for electricity production. This is due mainly to the costs of renewable energy technology. Also, for heating, fossil fuel-based equipment is the most sold and so the most used way for heat production. Until fossil energy sources are mainly used, we will be far from zero emissions and far from any climate change target.

Figure 3 - World gross electricity production by source in 2019. [10]

Figure 4 represents CSP worldwide projects – operational, under construction and in development phase. The biggest worldwide plant is present in Spain with 2304 MW of power. This amount of power is provided by a combination of plants made by parabolic trough plants, Fresnel technology plants, and parabolic cylinder hybridized with biomass. [11] In the Figure 5 is illustrated the need for additional CSP plants to be in track with SDS, which requires annual average growth of almost 24% through 2030. [12]

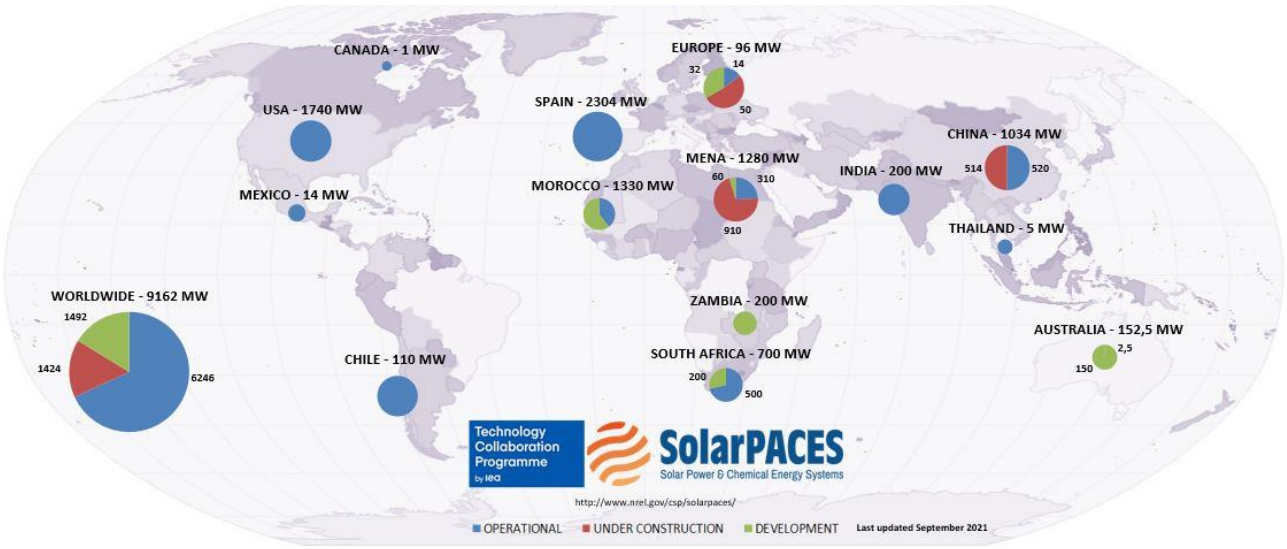

Figure 4 - CSP projects around the world. [13]

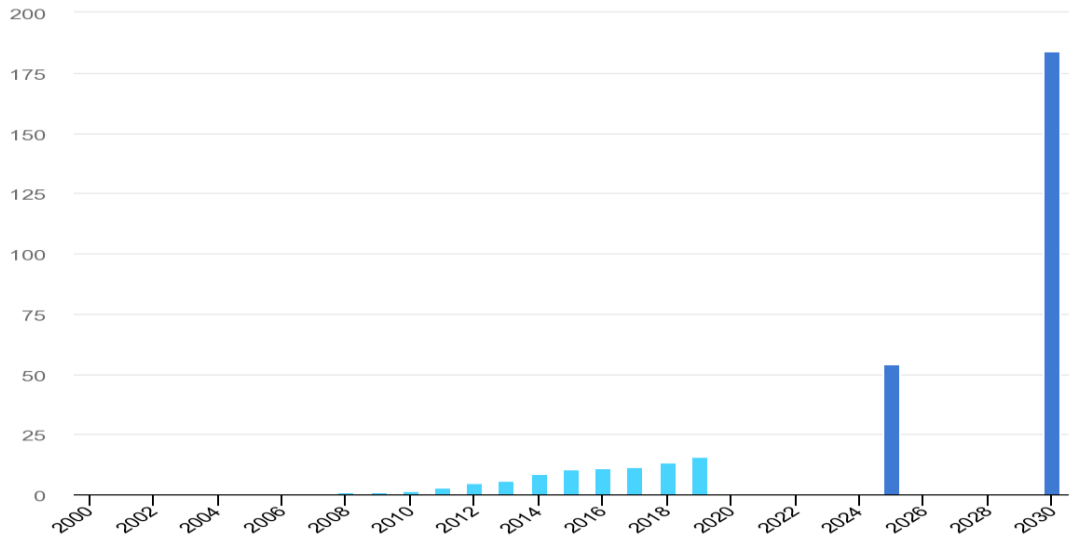

Figure 5 - CSP in SDS - IEA. [12]

2.2 Introduction to Concentrated Solar Power technology

Concentrating solar power systems use a combination of mirrors or lenses to concentrate direct beam solar radiation to produce high temperature heat. This heat can be used as process heat, for electricity or fuels production, or for desalination, by different downstream technologies. Commercial development of CSP technology started between 1984 and 1995, but then up to 2005 only research, development and demonstrations took place without any further commercial deployment. [14]

The CSP technology has been technology of interest since 7th century B.C. when glass was used to concentrate sun's rays to make fire and to burn ants. Then 212 BC when Archimedes described the idea of mirrored panels to concentrate the sun and, according to myth, to set fire to wooden enemies ships. In 1816 Robert Stirling built heat engines in his home workshop. This engine was later used in dish Stirling system for power production. In 1982 the U.S. Department of Energy begins operating a 10 MW central receiver demonstration project. Then, in 1986 the world's largest solar thermal facility was commissioned in California. Parabolic trough system was used to produce steam which powered a conventional turbine to generate electricity. [15]

Unlike PV technology, CSP systems are not able to use diffuse radiation, making them best suited to areas with a high percentage of clear sky and very high Direct Normal Irradiation (DNI). For this reason, in sunniest countries CSP can be expected to provide base-load power by 2025 to 2030. While on a worldly scale, this technology alone could provide 11.3% of global electricity. [16]

Up to now four main CSP technologies have been developed: Linear Fresnel, Parabolic trough Collectors, Parabolic Dish and Central Tower. According to the receiver and focus type the main technology families can be sub-grouped as described in Table 1.

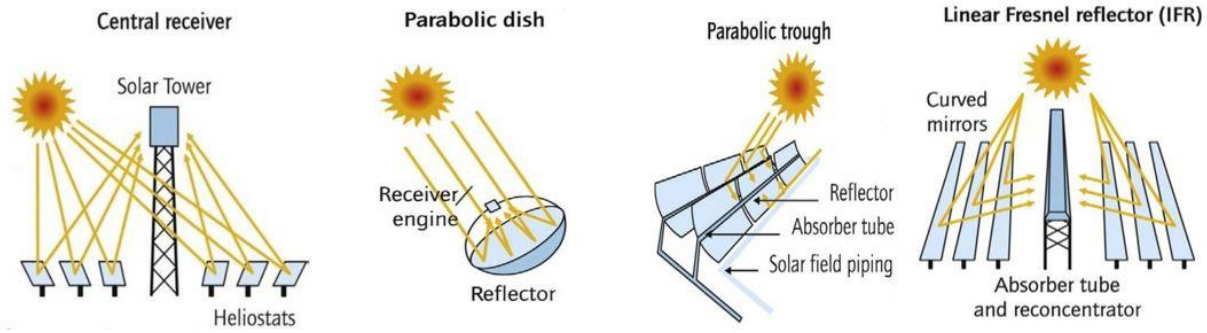

Figure 6 - Main CSP technologies. [17]

Table 1: CSP TECHNOLOGIES

	Line Focus	**Point Focus**
Fixed Type Receiver	Linear Fresnel	Central Tower
Mobile Type Receiver	Parabolic trough	Parabolic dish

Linear focusing systems concentrate the solar beams on linear absorber tubes or series of tubes. The reflectors are tracked about one axis to keep the sun's image focused on the absorber tube. This is also known as a single axis tracking technology. HTF, inside the tube, could be water, steam, or synthetic oil. Temperature range is between 350 °C and 550 °C. On the other hand, in point focusing systems all the concentrators would concentrate solar radiation at the central focal point. In this technology's operation temperature can reach up to 1300 °C. [15] In the following paragraphs four technologies will be described more in depth and then more attention will be put to Parabolic Dish Plants.

2.3 Linear Fresnel Reflector

Linear Fresnel Reflector (LFR) is a line focusing single axis tracking mirror technology. It has mirrors aligned along a north-south axis, able to track sun from east to west. [18] LFR is composed of many long row reflectors that together focus sunlight images that overlap on an elevated linear tower receiver running parallel to the reflector rotational axis. In this way a large size array can be built in an inexpensive way using similar or identical focal length glass mirror elements. The LFR receiver is fixed in space, and the reflectors rotate to keep focus on the fixed receiver. The reflectors are inclined at different angles because they have different positions relative to the tower target. In this way it is possible to build a large basic unit of identical relatively small reflector of long focal length, which allows the use of almost flat, lower cost glass mirror elements. [12]

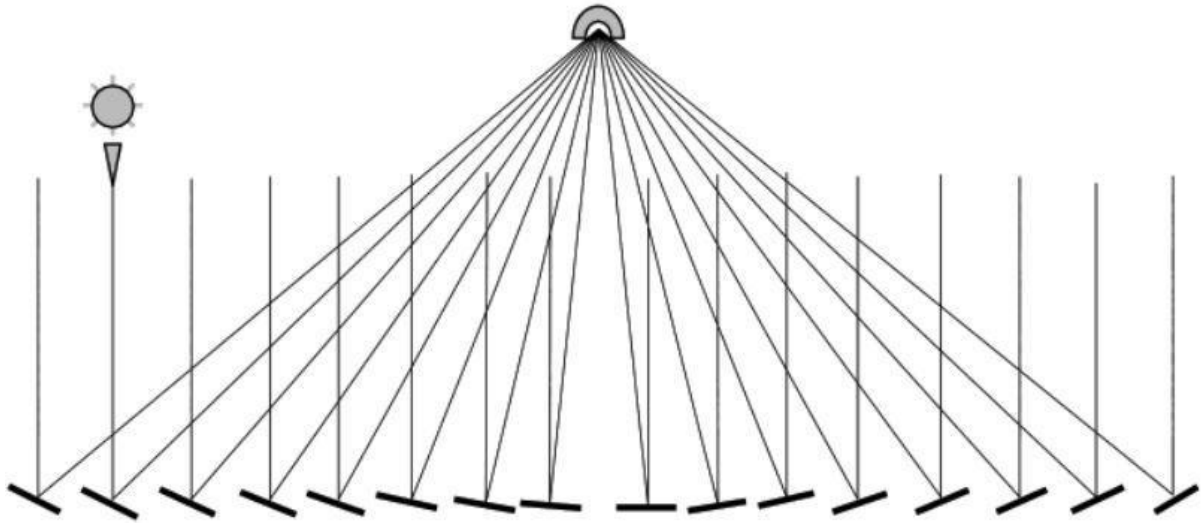

Figure 7 - LFR basic configuration seen from one end. Each reflector tracks the sun by turning about a horizontal axis normal to the page. [18]

2.4 Parabolic trough Collectors

Geometrically, the ideal reflectors to use with a single receiver are with parabolic or paraboloidal shape. Nevertheless, at large scale these become unwieldy and may require extensive structure to withstand wind loads. [19]

Parabolic trough collectors (PTC) are linear focus mobile collectors, with parabolic shaped concentrators with focus on the receiver. The solar radiation is concentrated on the receiver tube by a larger collector aperture area, heating the fluid that circulates through it. In this way, solar energy is transferred to thermal energy in the form of sensible or latent heat of the fluid. [20] In the case of synthetic oil as HTF the upper temperature of the thermodynamic cycle is limited at 400°C, and thus the maximum efficiency is limited to around 38%. On the other hand, recently Abengoa Solar is developing a test loop of certain molten salts to allows the CSP plant with PTC system to operate at 500 °C. [18] [21]

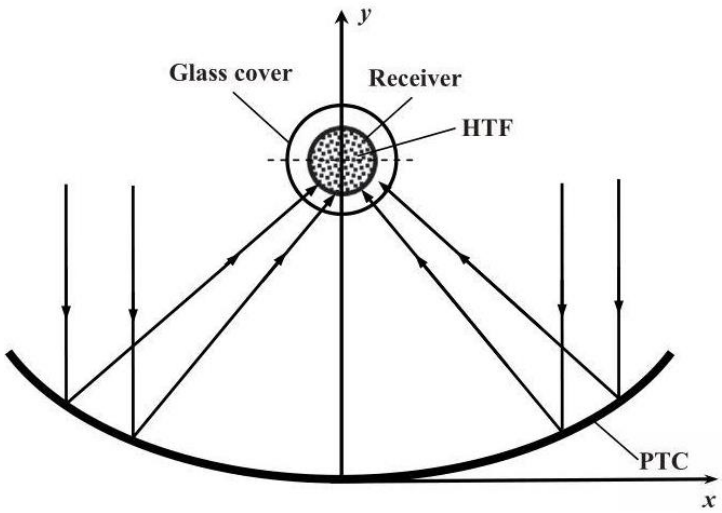

Figure 8 - Schematic of PTC with tube receiver. [21]

2.5 Central Tower

Central tower receiver system is made of an array of tracking mirrors, called heliostats, which are distributed in a field to avoid interference between them as they rotate to reflect incident direct – beam solar radiation on an elevated receiver or secondary reflector. Receiver absorbs incoming sunlight as heat at an elevated temperature. This energy is collected by HTF and can be stored as thermal energy, used to drive an electrical generator, or used as process heat. Receivers are often built as single large systems to power the steam cycle; however, small systems with single or multiple towers have attractions in several applications. In early system steam was used as HTF but nowadays molten salts are used which allow to reach temperatures up to 1300 °C. [22]

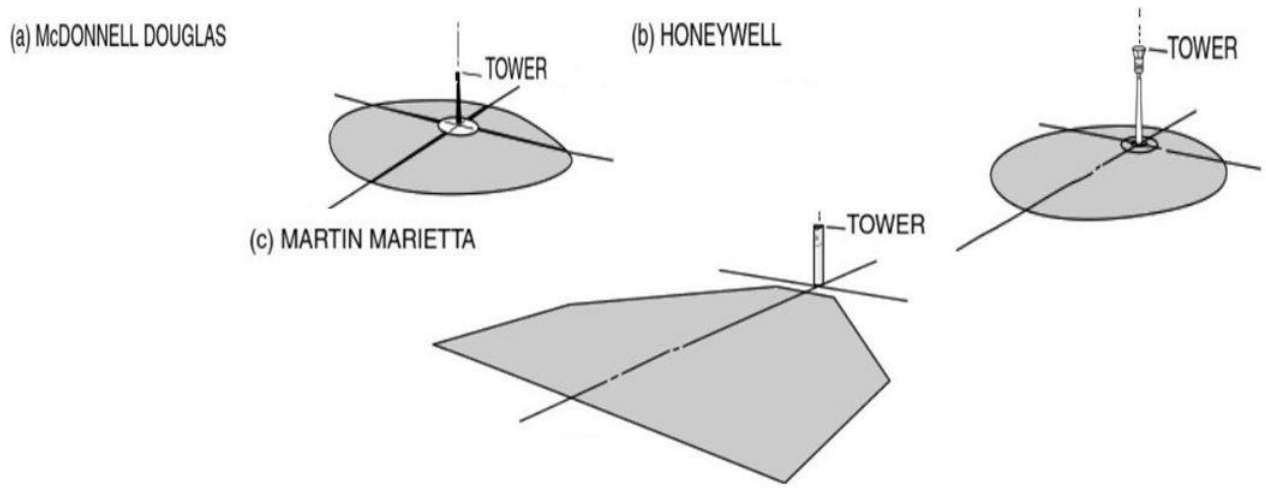

Figure 9 - Some of Central Tower CSP configurations. [22]

2.6 Parabolic Dish

Among several CSP technologies, hereby work analyses the receiver of a Parabolic Dish CSP system. Thus, this system will be presented with more details with respect to the previous cases.

Dish CSP systems focus solar energy into the receiver by paraboloidal mirrors. This energy is then transferred to a heat engine/generator or into a HTF that is transported elsewhere. Dish concentrators have the highest optical efficiencies, the highest concentration rations, and the highest overall conversion efficiencies of all the CSP technologies. [23]

John Ericsson is often acknowledged as the first person to couple a parabolic dish with an energy conversion system (the Stirling engine). Like many others, this renewable energy technology had the biggest investments after the oil crisis in 1973. In the 1980s the budgets for solar research were cut drastically as energy concerns dissipated but development effort continued with first commercialization during the 1990s. [24]

A dish system consists of: (a) a parabolic shaped concentrator, (b) tracking system, (c) receiver (solar heat exchanger), (d) an (optional) engine with generator and (e) a system control unit. [23]

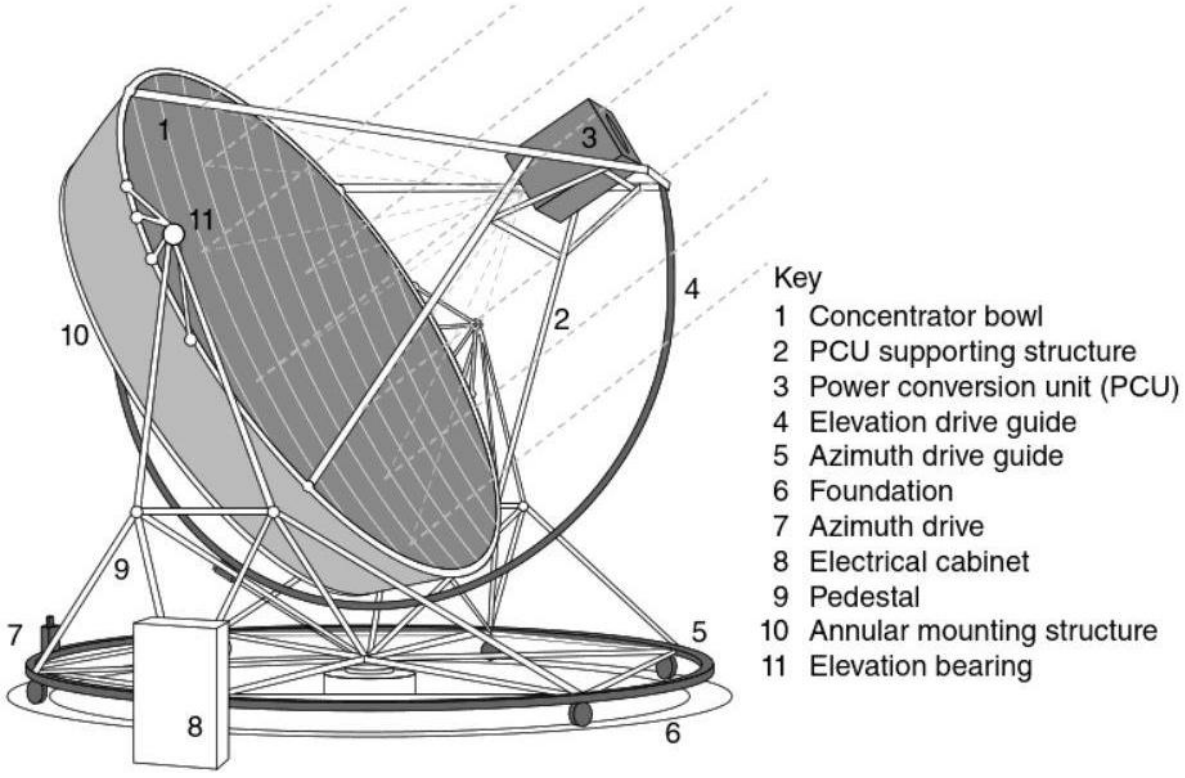

Figure 10 - Schematic representation of a dish system with azimuth – elevation tracking mechanism. [24]

2.6.1 Concentrator

Concentrator optical surface is a truncated paraboloid. It is a continuous, or faceted, mirrored surface with one focal point. [24] The performance of a concentrator is affected by solar irradiance incident on the concentrator, wind velocity, ambient temperature, mass flow rate of HTF, angle of inclination of the receiver from the horizontal plane, and so on. Main parameters for concentrator characterization are: [25]

Aperture area: it is the region where solar radiation is intercepted by the concentrator.

Stagnation temperature: it is the maximum achievable temperature inside the receiver which is obtained with a stagnant fluid, and it is used to evaluate the thermal performance of the solar collectors.

Acceptance angle: it is defined as the angle through which a source of light can be moved and still converge at the receiver. In case of continuous sun tracking, a small acceptance angle is essential, while with large acceptance angle only seasonal adjustment is necessary.

Cosine loss: are the reduction in reflected energy when the parabolic dish is not normal to the sun direction. As the optical axis of the solar parabolic dish always points toward the sun, cosine loss is zero.

Shading loss: as the receiver is located at the focal point of the dish, a portion of the reflective area of the dish is shadowed by it. Shading is minimized as the dish aperture area is quite larger than that of the receiver. Generally, this loss is less than 1%.

Reflectivity loss: are due to the imperfect reflectivity of the mirrors. A reflective surface with a low iron clear mirror coated with silver provides a reflectivity of 90% to 94%.

Transmission and absorption loss: transmission loss is the amount of energy lost in the air while reflected light is passing from dish to receiver surface. Likewise, absorption loss is the small fraction of reflected radiation absorbed by the receiver surface. Generally, the transmission and absorption loss is about 2% to 4% of total energy loss.

Absorber area: it is the total region of the surface of the absorber that gets the intense solar radiation.

Optical concentration ratio: the averaged irradiance (radiant flux) I_r integrated over the receiver area (A_r), divided by the insolation incident on the collector aperture. Optical concentration ratio relates directly to lens or reflector quality.

$$CR_o = \frac{\frac{1}{A_r}\int I_r dA_r}{I_o}$$

Geometric concentration ratio: the area of the collector aperture A_a divided by the surface area of the receiver A_r.

$$CR_g = \frac{A_a}{A_r}$$

Optical efficiency: it can be defined as the ratio of the energy absorbed by the receiver to the energy incident on the concentrator aperture area. The optical efficiency depends on the reflectivity, transmissivity, absorptivity, and shape of mirrors then, of tracking accuracy, shading effect, receiver-cover transmittance, cosine loss of the absorber, and solar beam incident effects. It values are usually in ranges between 0.6 and 0.7 and it can be evaluated by following mathematical correlation.

$$\eta_{opt} = \lambda\rho\tau\alpha\gamma cos\theta$$

Thermal efficiency: it is defined as the ratio of the useful energy delivered to the energy incident on the concentrator aperture.

$$\eta_{th} = \frac{Q_u}{Q_s}$$

Concentrator surface is usually made of reflective surface of aluminium or silver, deposited on glass or plastic. Silver glass mirrors are the most like the decorative mirrors used for domestic applications and they are also the most durable. Due to curvature because of short focal lengths of the dish concentrators, relatively thin glass mirrors are required. Furthermore, to improve the reflectance glass with low iron content is desirable. [25]

2.6.2 Tracking system

Tracking system is required to follow the path of solar energy by tracking the Sun's motion and collecting maximum solar radiation onto the collector throughout the day. This system can implement moving the concentrator of about two axes. [26] Two ways are possible:

- Azimuth – elevation tracking: with this mechanism the dish rotates in a plane parallel to the earth surface (azimuth) and around an axis perpendicular to it (elevation). In this way the collector can rotate up/down and left/right.
- Alternatively with polar – equatorial tracking method: in this case the collector rotates about an axis parallel to the Earth's axis of rotation at a constant rate of 15 $\frac{^\circ}{hr}$, the same rotation rate of the Earth's and, about the declination axis. This second axis is perpendicular to the polar axis and movement around this occurs slowly and varies by ± 23½ ° over a year. [23] [24]

Passive tracking system has also been developed. It is based on differential heating of two interconnected tubes which are filled with the gaseous refrigerants. It has been developed in absence of microcontrollers, motors, and gears. [27] [28]

2.6.3 Receiver

Reflected energy by the concentrator is absorbed by the receiver and transferred to the working fluid.

Direct steam generation receivers are generally used for small, off-grid engines and for large, on-grid steam power plants. Direct steam generation receivers are typically single pass coils that form a cavity. A thermal efficiency of 93% for a 500°C at the outlet was obtained for a trapezoidal cavity at White Cliffs in Australia. While ANU SG4 Big Dish steam receiver achieved 97.1% of thermal efficiency in on-sun tests for steam >500°C. [24]

In case of cavity type receiver, the solar radiation is concentrated at the small opening where inside it impinges on tubes carrying the working fluid. With this type of receiver only a small amount of incoming radiation is reflected to the atmosphere through inlet aperture while thermal radiation and convection loss is minimized.
Cavity receivers were used, for example, for dishes in the Solar Total Energy Project at Shenandoah in Georgia. The plant operated between 1982 and 1991. The receiver had a stainless-steel coil – type heat exchanger where the oil was heated to 399°C and used to generate steam for powering a Rankine steam turbine. [24]

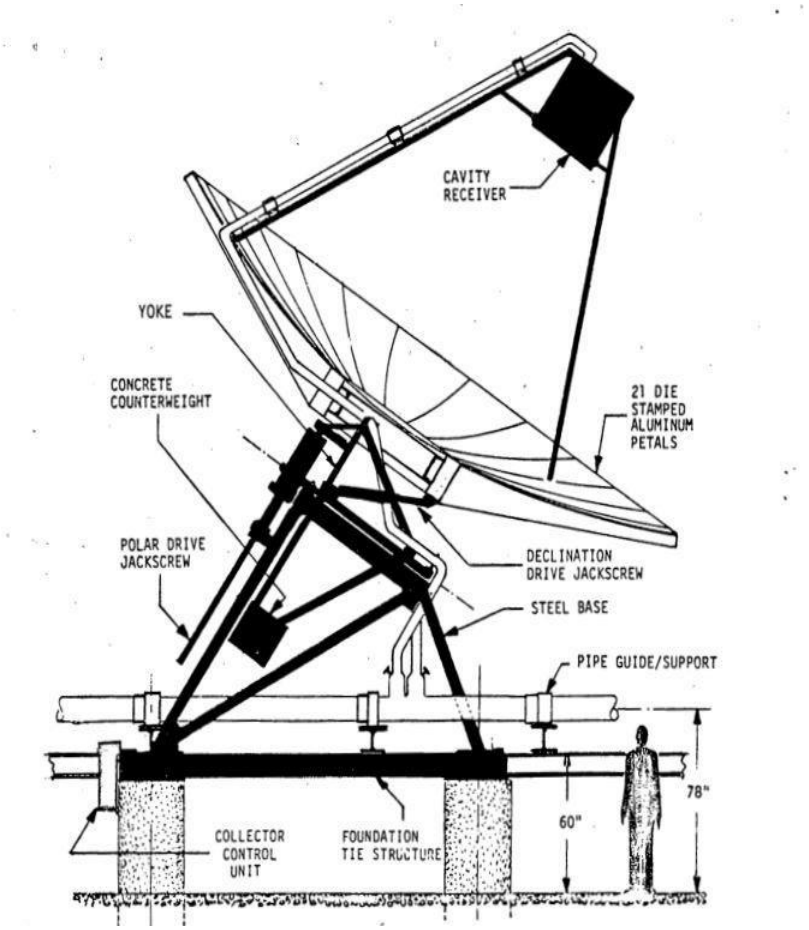

Figure 11 - Schematic view of the Shenandoah dish system. [29]

Another example of cavity receiver use in a parabolic dish system is the PDC – 1 dish designed by the General Electric (GE) company. It was a cavity type, direct heated, once – through monotube boiler with toluene at supercritical pressure. It was formed by cylindrica copper shell and back wall with stainless steel tubing brazed to the outside surface, surrounded by insulation. The receiver, designed in 1982, reached thermal efficiency of 95.2%. [30]

Volumetric receivers are also used in parabolic dish CSP technologies. This kind of receiver is composed of porous structures (absorber matrix). Through this structure concentrated solar radiation penetrates within the absorber volume while the HTF passes under a forced convection flow regime. A fraction of radiation gradually absorbed by the solid structure is transported as thermal energy to the HTF by convection. With volumetric heating higher energy conversion efficiency can be obtained with respect to surface heating, as in tubular receivers, as higher absorber temperatures can be displaced in the interior of the receiver pore structure. [29]
Porous absorber structure allows the use of air as HTF despite its low heat transfer coefficient. This technology has been developed since the early 1990's. [31] Thermal reradiation losses are reduced since there is a large temperature difference between HTF and absorber material at the entry of the absorber which lowers the material temperature of the volumetric absorber. If the temperature of the front of the absorber sinks below the HTF outlet temperature, then this is described as the "volumetric effect". [32] Volumetric receiver was used in a dish developed by US company Omnium – G which was installed in Colorado in 1978. Air was used as an HTF, and it was heated up to 980°C. Air could be heated far higher but the limitations lie in the receiver material and other components of the plant. [22] [32]

2.6.4 Engine

For conversion from thermal to electrical energy, Stirling engines nowadays are used in most of the dish systems since they have high efficiency (thermal to mechanical efficiency can exceed 40%), high power density and potential for long-term low maintenance operation. [23] [27]

3 Thermal Energy Storage

The foremost weakness in renewable energy systems, such as wind or solar farms, is related to their availability during the 24 hours of a day or different times of a year. This problem can be solved providing a backup boiler to compensate for the unavailability of RES and using thermal storage mediums, such as PCM. The boilers are usually fed by fossil fuel resources while TES require high initial investment. The possibility of integrating cost – effective local storage capacity is one of the most distinct advantages of CSP over other RES technologies. In a TES systems energy is supplied to a storage system to be used later, involving three steps: charge, storage, and discharge.

The main requirements for the design of a TES system are high energy density in the storage material, good heat transfer between the HTF and the storage material, mechanical and chemical stability for the storage material, compatibility between the storage material and the container material, complete reversibility of several cycles, low thermal losses, and easy control. The most important parameters for the design are the operation strategy, the maximum load needed, the nominal temperature and, the integration into the whole application system. [33]

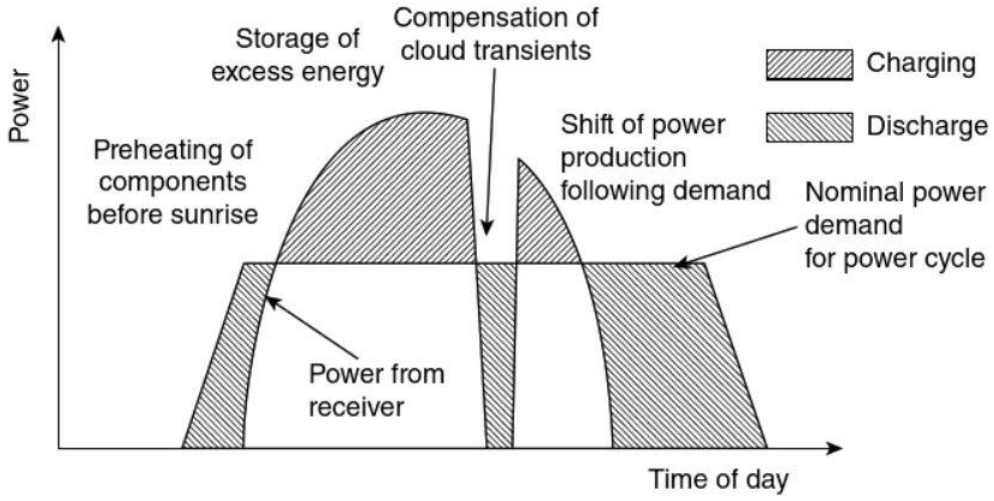

Figure 12 - Various function of TES in CSP plant. [34]

TES systems can be classified in three different categories: sensible, latent and thermo – chemical energy storage.

3.1 Sensible Heat Storage

The heat storage based on temperature increase of a given material is referred as sensible. Sensible TES usually store energy within rocks, gravel, water etc. by raising the temperature level.

The amount of energy stored in a sensible TES is calculated as expressed in the following equation:

$$Q = m \cdot c_p \cdot (T_2 - T_1) = \rho \cdot V \cdot c_p \cdot (T_2 - T_1)$$

Where Q is the amount of heat stored in the material [J], m is the mass of storage material [kg], c_p is the specific heat of the storage material [J/(kg·K)], and ΔT is the temperature change [K]. Depending on the specific heat capacity, the same amount of energy can heat the same mass of another material under larger or lower temperature differences. The specific heat values can vary by several orders of magnitude, and it depends on the storage material.

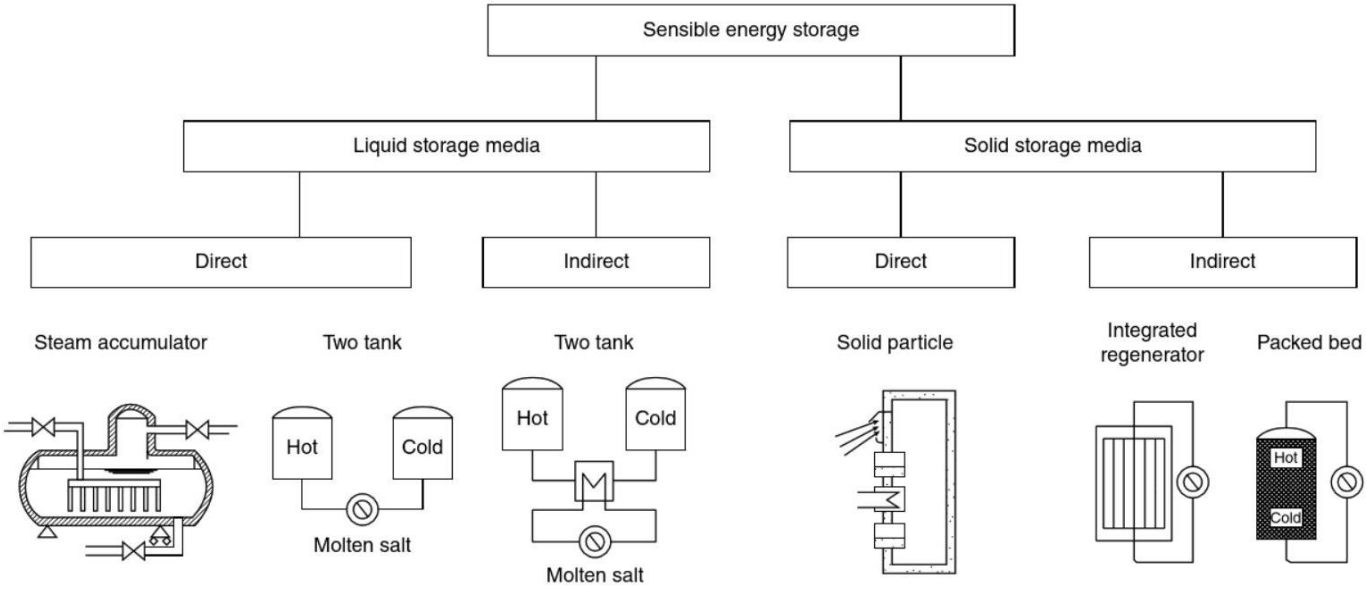

Figure 13 - Concepts for sensible TES. [34]

3.2 Latent Heat Storage

Latent heat storage systems use a phase change of material to store energy. The latent heat is the energy necessary for phase change and in general it is greater than sensible heat. The phase change of interest for common purposes is the liquid – solid as they occur under acceptable specific volume variations. The heat stored in that kind of system can be expressed as in the following equation where c_l and c_s are the heat capacities of the liquid and solid phase, Δh_{pc} is the head absorbed during the phase change per unit mass [J/kg] and T_{pc} is the temperature of the phase change process.

$$Q = m \cdot \int_{T_{start}}^{T_{pc}} c_s(T)dT + m \cdot \Delta h_{pc} + m \cdot \int_{T_{pc}}^{T_{end}} c_l(T)dT$$

The first term represents the heat stored thanks to the sub – cooling of the soldi phase at the beginning of the process, the second term the total heat absorbed during the phase change and the third one is the heat obtainable thanks to the super – heating of the liquid phase.

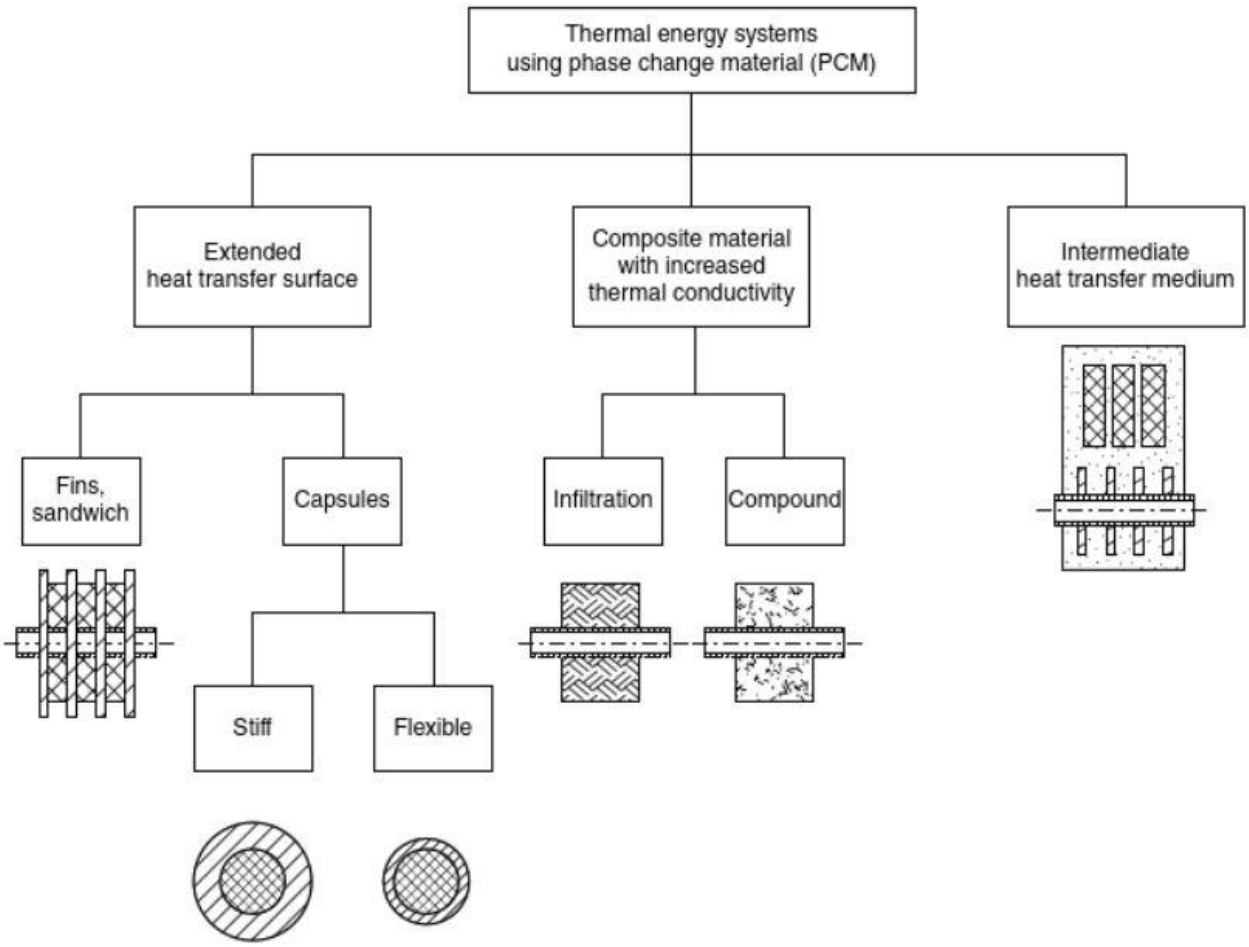

Figure 14 - Latent TES configurations. [34]

The development of a latent heat storage systems starts with the selection of the PCM. Main PCM characteristics are melting temperature [°C], density [kg/m^3], thermal conductivity [W/mK], heat of fusion [kJ/kg], volume specific latent heat [kWh_{th}/m^3], capacity specific media cost [\$/kWh_{th}].

In the following figure is represented generic classification of such materials.

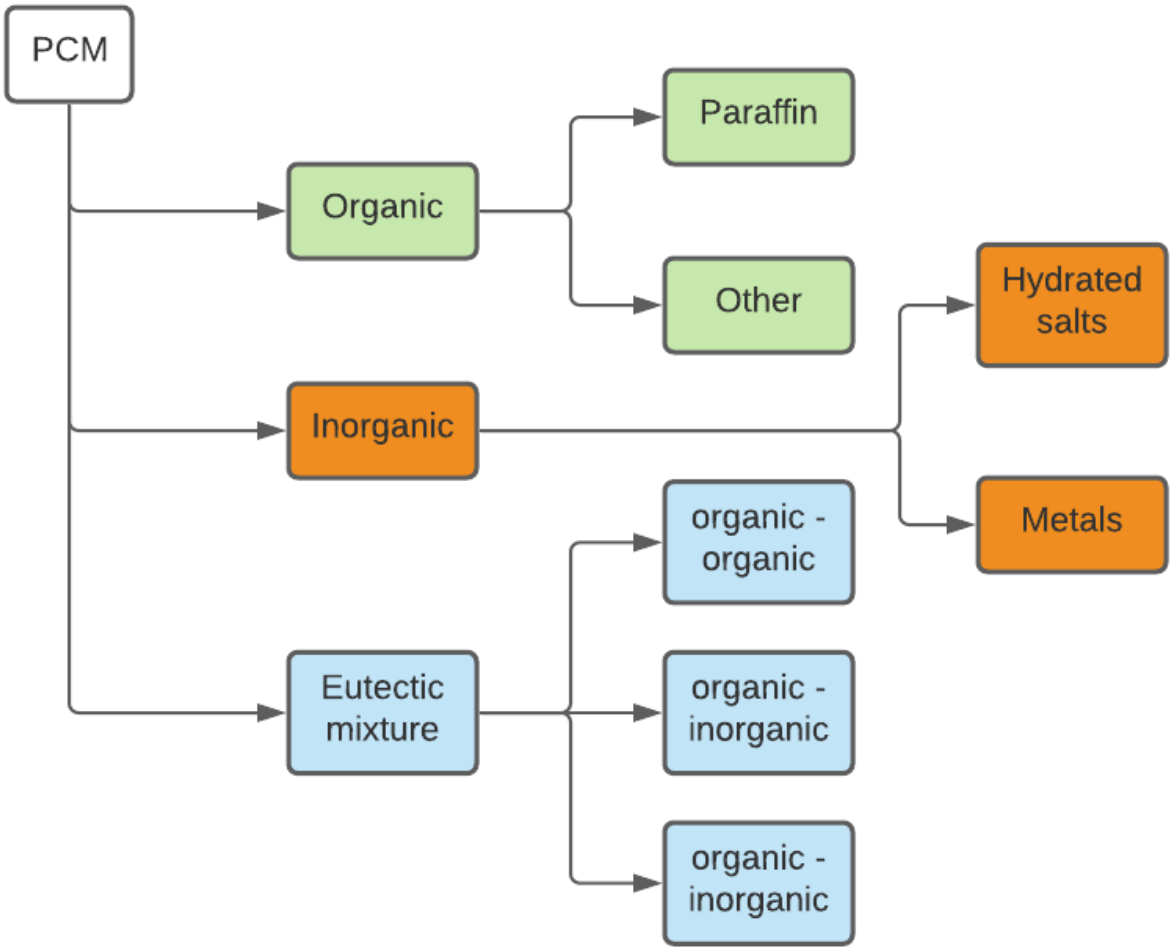

Figure 15 - PCM classification.

When using finned tubes, to extend heat transfer area, in a PCM storage the distance between parallel tubes is larger than that of conventional heat exchangers, the material of the fins must be corrosion resistant in a PCM environment and the fins must be able to withstand thermomechanical stress due to volume variation of the PCM. Optimal materials used for the fins are aluminium or graphite, due to their high thermal conductivity and lower volume specific cost with respect to steel. The temperature range of this materials is limited in case in which nitrates are used as PCM by corrosion resistance (<400°C for aluminium, <250°C for graphite).

To increase heat transfer area the macro – encapsulation of PCM is another option. A significant drawback of this configuration, for CSP technology, is the necessity to use a gas volume to compensate for the expansion of PCM during melting.

To avoid oversizing of a heat exchanger area, an intermediate heat pipe system, based on evaporation and condensation of a suitable intermediate HTF can be used to transfer energy between a heat exchanger and the PCM. The intermediate heat transfer fluid should undergo a phase change between the liquid and gaseous state. During the charging process the secondary fluid in the heat exchanger evaporates and condensate in contact with the PCM, melting it. During the discharging process the PCM solidifies while the intermediate heat

transfer fluid condensates in the heat exchanger giving heat to the main heat transfer fluid. [34]

3.3 Thermo – chemical Heat Storage

In thermo – chemical heat storage the energy is stored in form of chemical energy using a reversible chemical exothermic/endothermic reaction. Usually, chemical energy conversion has better energy storage performance efficiency than physical methods (sensible and latent heat storage). The most important challenge is to find the appropriate reversible chemical reaction for the energy source used. [33] The storage mechanism can be described with the following equation:

$$A_{(s)} \underset{heat\ storage\ endothermic\ reaction}{\overset{heat\ release\ exothermic\ reaction}{\rightleftharpoons}} B_{(s)} + C_{(g)}$$

During the charging process (endothermic reaction), the solar energy is used to move the reaction from the solid reactant (A) to the solid ang gas product (B and C) which are stored separately. When a discharging is required (exothermic reaction), B and C are placed in contact to react and release the chemical reaction energy stored. [33]

4 Presentation of the system

First part of the thesis is focused on the analysis of solar concentrator. The goal is to determine the temperature that can be reached in the focal point with medium value of irradiance. Knowing this temperature level, it will be possible to determine the appropriate materials for the receiver and to quantify energy production.

To perform this analysis COMSOL Multiphysics 5.4 is used. In particular, the Ray Optics module present in the COMSOL library is used. With this function the geometry is divided in two parts: one part is represented by the parabolic concentrator while the other is the cylindrical receiver.

The parameters used inside the Ray Optics module are those of parabolic concentrator present at Energy Center Lab at Politecnico di Torino. In following table are reported parameters of parabolic concentrator used in this simulation.

Table 2 - Geometrical characteristics of solar colector

	Symbol	Value
Rim angle	φ	0.9028 rad
Focal length	**f**	0.92 m

Knowing these two parameters, concentrator diameter and area are obtained using following formulas:

$$d = 4 \cdot f \cdot [\csc(\varphi) - \cot(\varphi) = 1.78\, m$$

$$A = \frac{\pi \cdot d^2}{4} = 2.50\, m^2$$

The receiver in this first simulation is the cylindrical one placed at the distance from concentrator that is equal to the focal length. The receiver has radius equal to 50 mm and height equal to 100 mm.

4.1 COMSOL model – Temperature and Power evaluation

System concentrator – receiver is built using a built – in Part from the Part Library of Ray Optics Module. The Ray Optics Module provides tools for computing ray trajectories, intensity, and polarization. To compute the Geometrical Optics interface the following conditions must be met: [35]

- At least one release feature to specify the initial position, direction, and intensity of rays.
- Boundary conditions that determine the way in which rays interact with their surroundings.
- Ray proprieties, used to specify the frequency or free – space wavelength of the rays.
- Medium properties, used to specify the refractive indices of the media through which rays propagate.

In addition to the listed requirements, the Geometrical Optics interface includes tools for coupling the results to other physics interfaces. Node called Accumulator can be used to transfer information from rays to the domains they pass through or the boundaries they hit.

The aim of the first simulation is to evaluate the temperature and the power that can be reached at the focal plane of the system. The focal plane is the surface of the receiver that is looking towards the solar dish. Average solar irradiance is assumed to be equal to 800 W/m^2

In the following Figure 16 is represented the Paraboloidal Reflector Shell 3D from the COMSOL library that has negligible thickness. The whole model was built by following Ray Optics Module Manual and Solar Dish Receiver guide application builder available online. [36]

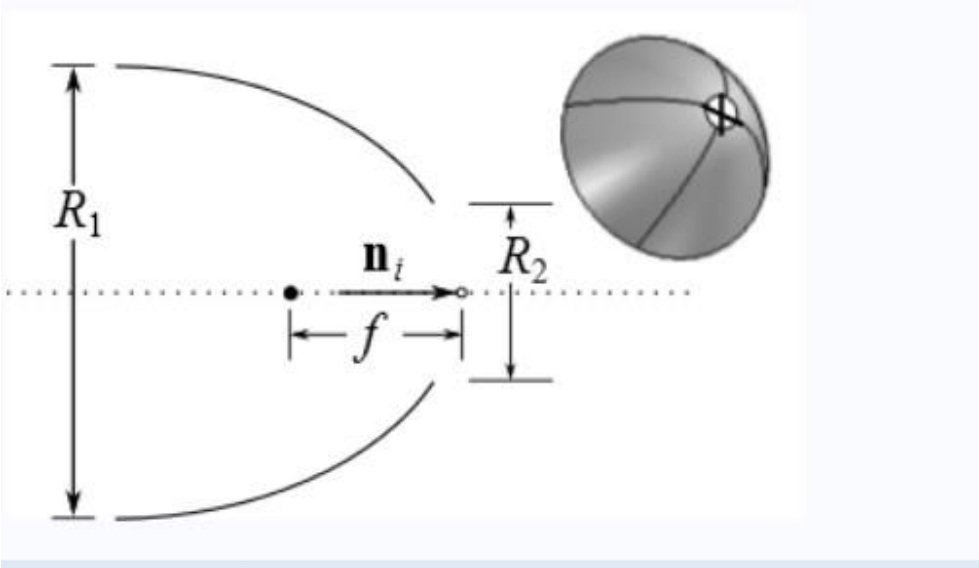

Figure 16 – Paraboloidal Reflector Shell 3D. COMSOL library

The whole system reflector – receiver is represented in the following Figure 17.

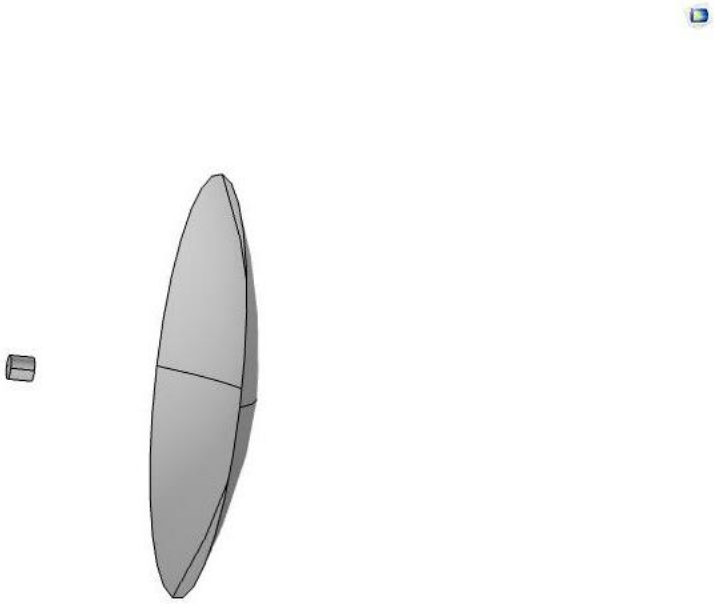

Figure 17 – System representation inside COMSOL software.

If the dish was a perfect reflector, meaning that all the incoming radiation was reflected specularly, the dish was perfectly smooth and the rays from the sun behaved as planar waveforms from an infinitely distant point source, all the incoming rays would be focused on a single point on the collector – at the focus of paraboloid. However, to make the system more realistic, this model considers several deviations from the idealized case:

- Some of the incoming radiation is absorbed by the dish itself. Even a newly installed dish absorbs a significant fraction of the incident radiation, and part of the dish can degrade over the course of its lifetime, reducing its efficiency. In this model the absorption coefficient is set to 0.1, meaning that 90% of the incoming radiation is reflected.
- An additional correction is included due to the finite size of the sun. Not all incident rays will be parallel; instead, the incident rays are sampled from a narrow cone with maximum angle, ψ_m, of 4.56 mrad. In practice, some radiation is also emitted from the circumsolar region surrounding the solar disk, instead of the solar disk itself, but this radiation is neglected in the present model; that is, a circumsolar ratio (CSR) of zero is assumed.
- Since the surface of the dish is not perfectly smooth, the reflected rays are not all released at the exact direction. Instead, the surface normal is perturbed by an additional angle that is sampled from a Rayleigh distribution. This optical error is considered with a surface slope error of 1.75 mrad, that is the default value set by COMSOL.
- The limb darkening effect is built-in COMSOL and it considers the variation of power in rays coming from different regions of the Sun. In particular, the rays that are emitted from the center are more intense when compared to the rays emitted from the peripherical regions of the solar disk.

A dedicated boundary condition called *Illuminated Surface* is used to release rays directly from the surface of the dish, initializing their directions as if they were reflected from a

distant plane wave source. To each ray released is also assigned a fixed power based on the *Source power* setting for the *Illuminated Surface* feature. In this case, total source power is equal to $P_{src} = A \cdot I0$ where A is the dish projected surface area while $I0$ is the average solar irradiance set equal to 800 W/m^2 As the applications of geometrical optics involve plane or spherical waves that reflect off a large surface, then continue to interact with other nearby objects, the *Illuminated Surface* feature allows to reach a reduction in computational time by 50% if compared to some other methods. [35]

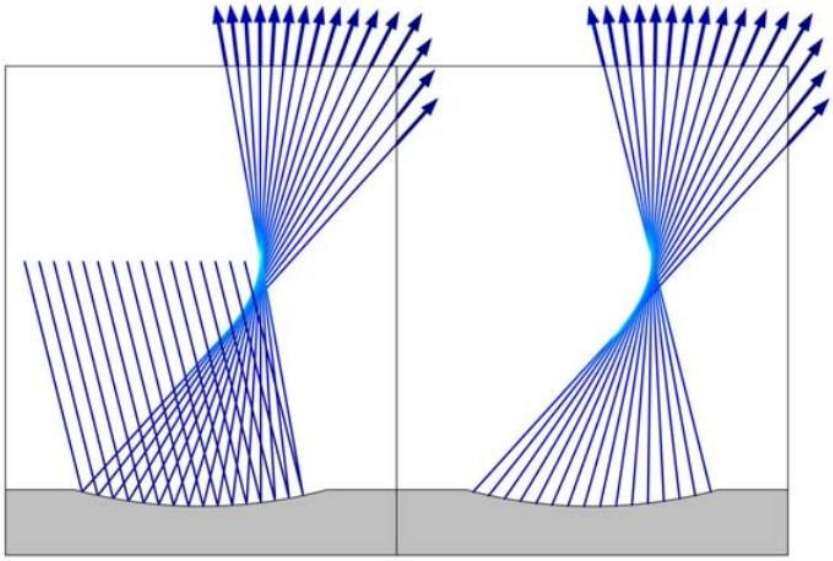

Figure 18 - Comparison of the ray trajectories and intensity when sending rays at a wall and using a Bounce condition (left) and using the Illuminated Surface feature (right) [35]

When the rays reach the surface of focal plane, they are stopped by the *Wall* feature. The node Wall is used to determine what happens to the rays when they met a boundary.

The *Deposited Ray Power* sub feature computes the incident heat flux in the focal plane.

The model includes two studies, each for different instance of Illuminated surface – real and ideal case. For each study rays are released from 250000 distinct points. At each point the incident ray direction is perturbed by a random angle. Real case includes the perturbed parameters listed above.

When rays reach the boundaries of geometric entities in a model, they do not interact with an exact parametrized representation of the geometry. Instead, they propagate through the mesh elements that discretize the modelling domain and interact with the boundary elements that cover the surfaces of the geometric entities. For this reason, a mesh must be present on any boundary that the rays may interact with. In addition, any domains in the selection for the *Geometrical Optics* interface must be meshed.

In a major part of cases the suitable mesh requires a good resolution on the curved surfaces. While the mesh within on flat surfaces may often be very coarse, the mesh on boundaries with small principal radii of curvature must be fine enough so that the direction of the surface normal can be determined accurately. This is needed as the curved geometry usually incur a significant amount of discretization error when predicting how rays will interact with them. The time and location at which the ray interacts with the boundary mesh might be slightly different from the time at which it would have interacted with an exact

representation of the surface. Having fine mesh on the curved surfaces improves the accuracy of the reinitialized wave vectors of the reflected and refracted rays. To reduce the mesh size on curvature surfaces without creating an unnecessarily fine mesh elsewhere, the Curvature factor in the *Size* setting can be reduced. In this work a *Curvature factor* of 0,2 was selected. Additionally, as the main goal is to determine the temperature evolution along receiver, a personalized *Free Triangular mesh* was used for this component with maximum element size equal to 2E-4 [mm] and minimum element size equal to 4E-5 [mm]. These measures were selected, after many attempts, as a compromise between accuracy and computational duration.

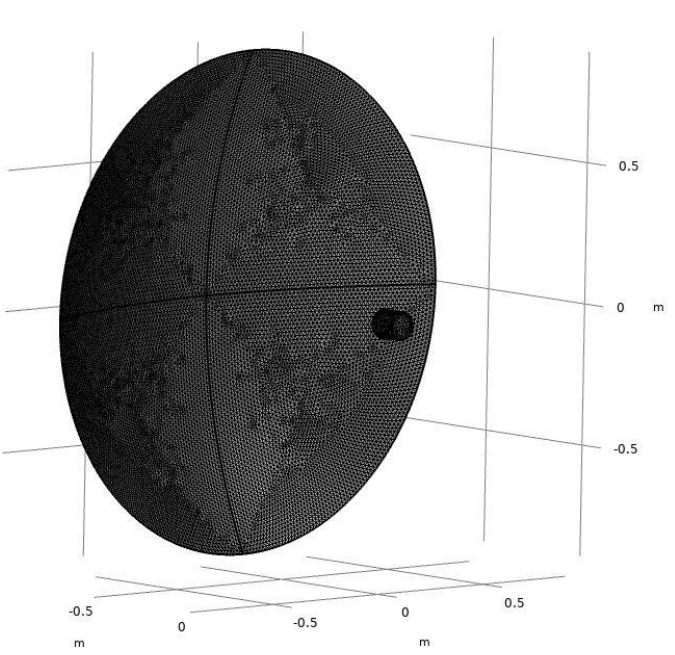

Figure 19 - Mesh representation

The ray trajectories emanating from the solar dish can be seen in the Figure 19 for Ideal and in the Figure 20 for real case conditions.

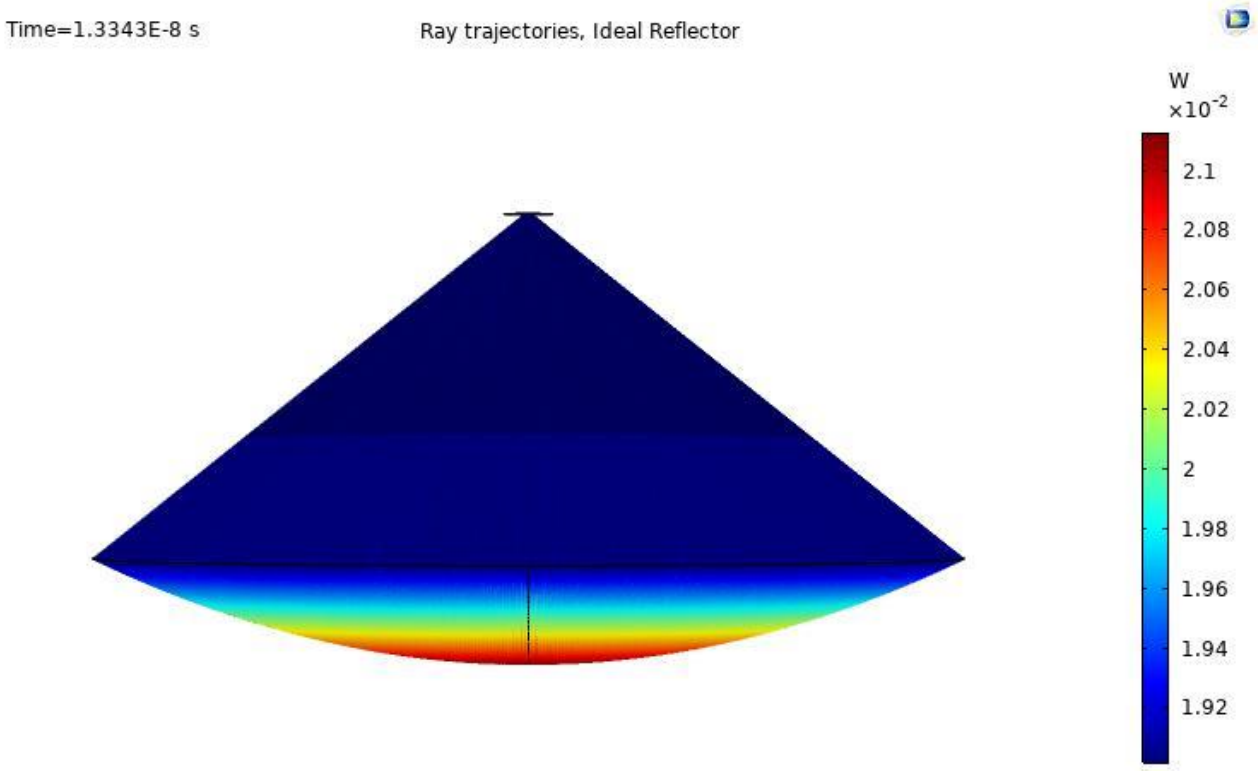

Figure 20 – Ray trajectories for ideal case solar dish.

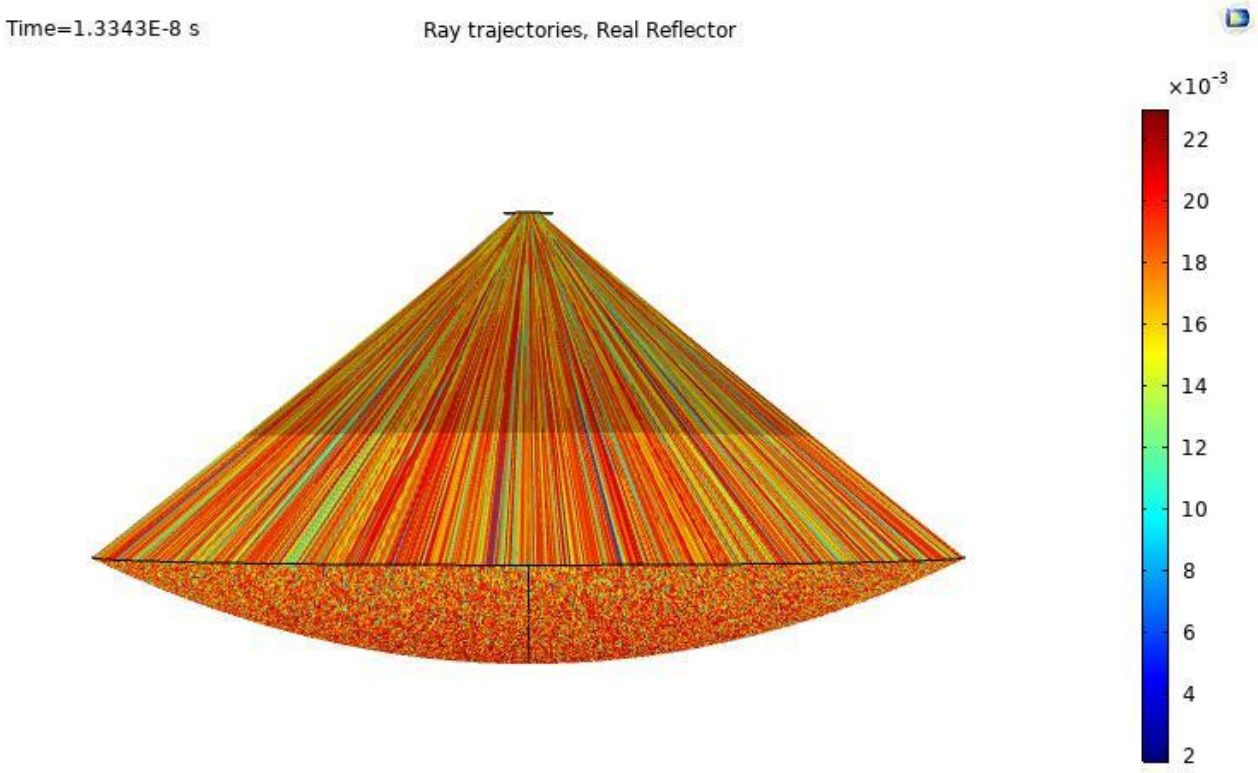

Figure 21 – Ray trajectories for a real case solar dish – including surface roughness, absorption, and solar limb darkening.

The results show that when the dish surface is completely ideal and has no slope error, the sun's rays hit the surface of the dish and are reflected very regularly at a point in the cavity space. For real dishes with surface slope errors, the sun's rays cannot concentrate on a point at the cavity space and for greater slope errors of the dish surface, the sun's rays are concentrated more irregularly near the receiver aperture.

Results show that when the surface of the dish collector is wavy, the reflected rays don't concentrate regularly inside the cavity receiver and some of the rays are reflected outside the space and cannot be absorbed by the receiver. The corresponding asymmetric and non – uniform distribution of solar flux on the inner wall of the receiver for an ideal and real dish with different surface slope errors is shown in the following figure. The obtained data for solar flux distribution show that the dish surface error has a substantial impact on the distribution and the amount of the reflected solar flux on the receiver walls, and consequently the overall performance of a dish reflector.

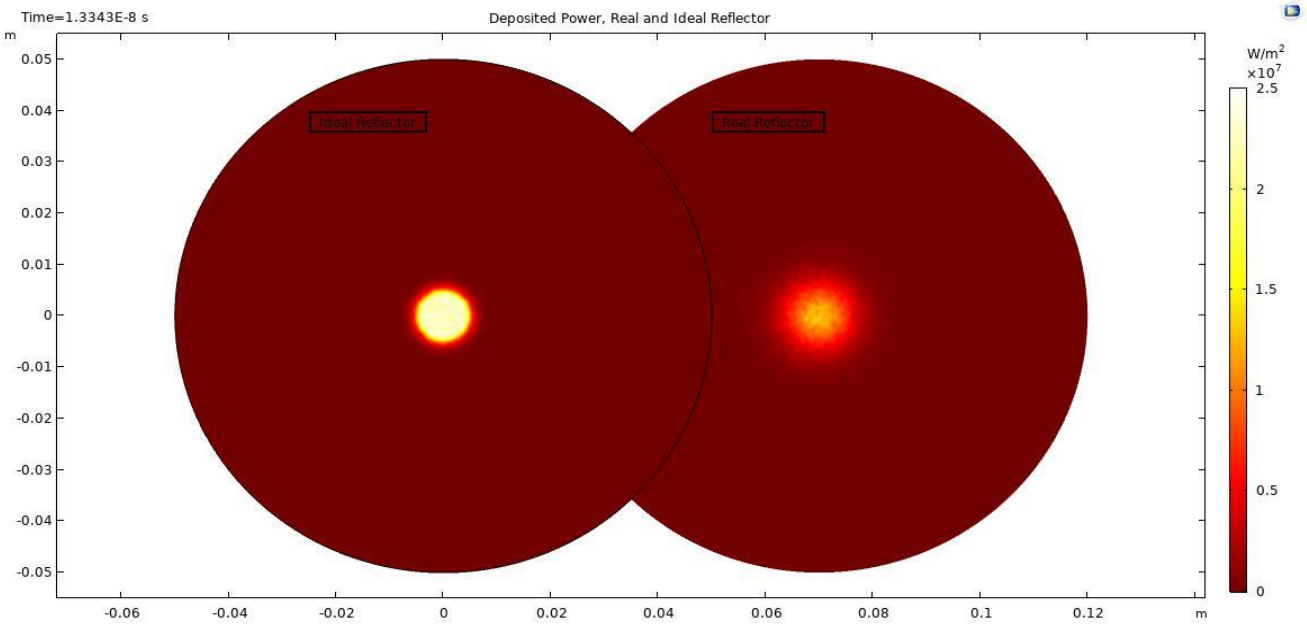

Figure 22 – Deposited power on focal plane in case of ideal and real reflector.

Surface maximum heat flux, evaluated by COMSOL sub feature *Average* of *Derived Values*, for ideal case is equal to around 26 W/mm² while in real case it is reduced to 14.6 W/mm².

These heat flux causes extremely high temperature on the focal plane. Temperature distribution on the focal plane is represented for the real case only. As we can see from the following Figure 22 the peak temperature is around 4000 K. The temperature is obtained by using the Stefan-Boltzmann law for a black body.

$$T = \left(\frac{q}{\sigma}\right)^{0,25}$$

Where q is the deposited power on the focal plane while σ is the Stefan-Boltzmann constant which is equal to $5{,}67 \cdot 10^{-8} \frac{W}{m^2 K^4}$.

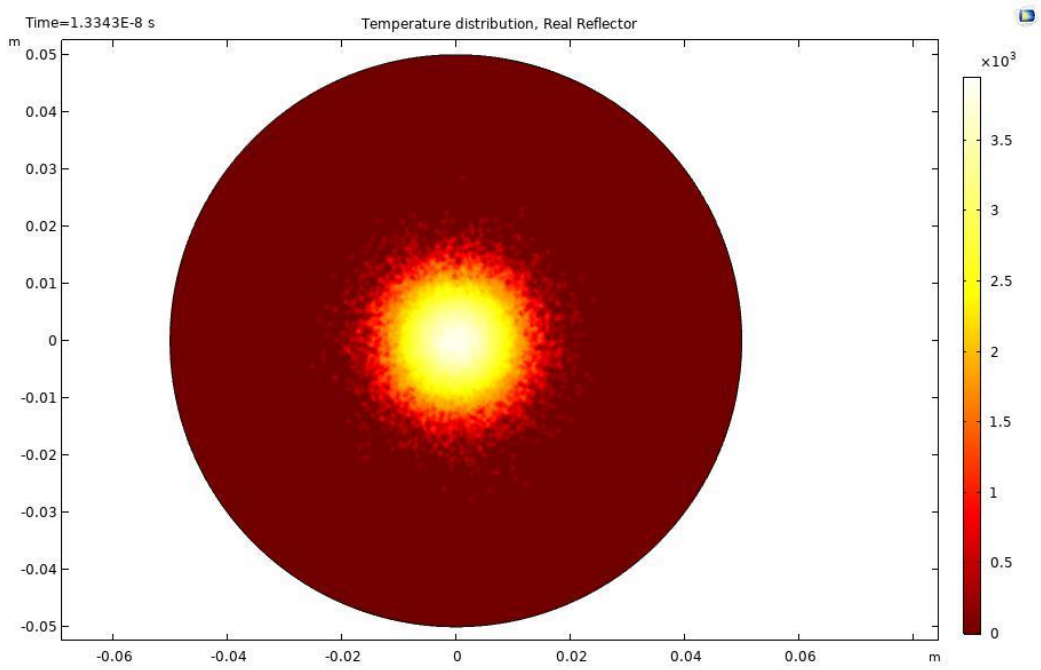

Figure 23 – Temperature distribution on the focal plane.

This extremely high temperature is reached as the receiver has still an optimal design even if some deviations for ideal case were introduced. The next step is to upgrade the geometry of the receiver and to design it as realistic as possible with the goal to reduce the peak temperature.

4.2 Receiver design

The aim of the next simulation is to include a more realistic receiver geometry design to determine a more realistic temperature inside the component, as the temperature previously obtained, for the flat plate receiver, was extremely high.

Cavity solar receivers for solar dish system could be cylindrical, elliptic, conical, or spherical and hetero-conical. These shapes allow to drastically reduce the convection losses however, by using selective coating thermal losses due to radiation can be reduced even more. According to some experimental studies, heat losses from a solar cavity receiver were less when compared with those occurring in the other type of receivers. [37] In this analysis cylindrical cavity geometry is used with inner coil heat exchanger. This kind of heat exchangers are simple and easy to manufacture and a real case example is reported in the following figure 24.

Figure 24 - Cylindrical cavity receiver [38]

In this new scenario the focal plane will be completely different with respect to the previous one. For what concerns reflector, the real case configuration from the previous paragraph is used.

After interception, the radiant flux impacts the receiver inner surfaces, the sides, and the bottom. When the radiant flux impacts a given surface, a fraction of it is absorbed, and the rest is reflected to the other surfaces, including the aperture. If it is reflected to the receiver wall, this process is repeated. If it is reflected to the aperture, this fraction of radiant energy is lost to the ambient – reflection losses. The reflection losses and the reflection on the receiver surfaces depend on:

- The receiver shape and size
- The solar absorptance of the receiver inner surfaces
- The reflection type of the receiver inner surfaces, namely specular, specular with Gaussian scattering or Lambertian (Diffuse).

So, to the factors introduced in the previous chapter to make the model more realistic, there are also this additional three. As a result, the heat flux absorbed by the receiver is not

uniformly distributed within the receiver inner surfaces and the actual distribution of the absorbed radiant flux density is determined by those factors.

New focal plane will be the inner cylinder with a radius equal to 115 mm and a height of 230 mm. The obtained temperature distribution is shown in the following Figure 25.

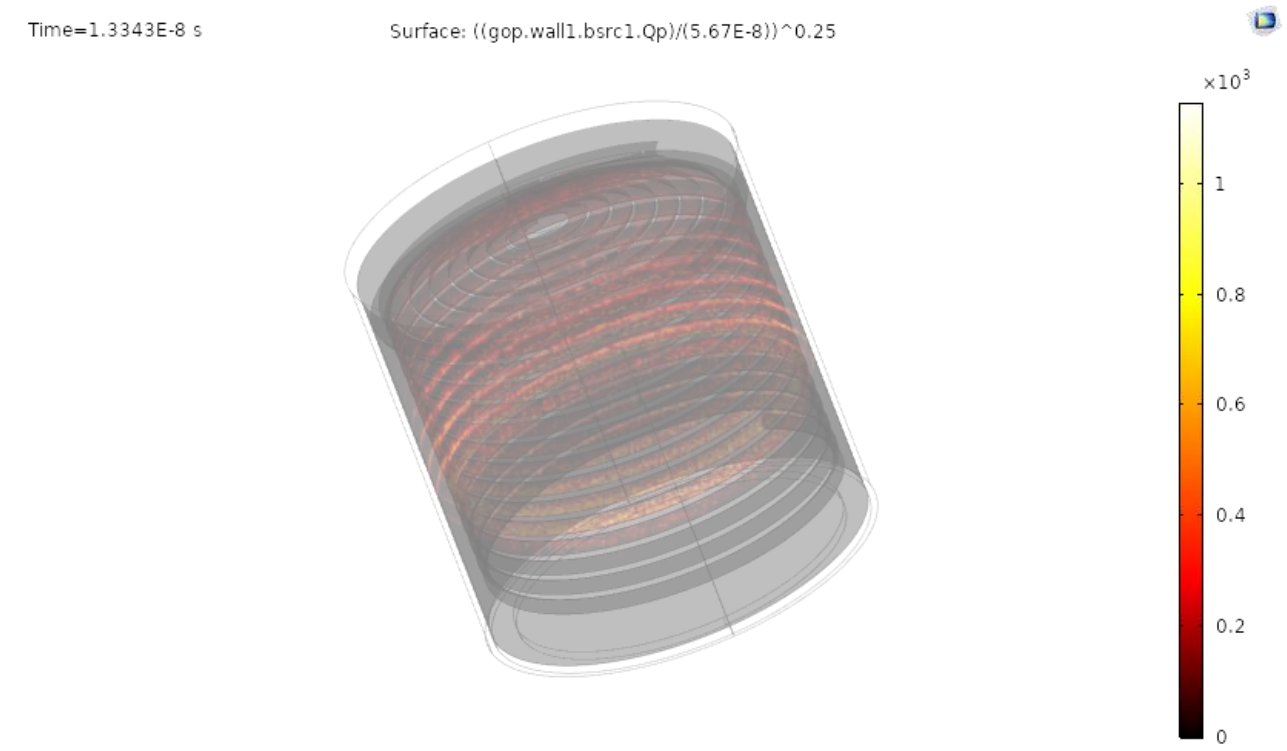

Figure 25 – Temperature distribution inside the cavity receiver [°C].

Maximum reached temperature inside the receiver is equal to 873,75 °C (1146,9 K) while the average power is equal to 7466,7 $\frac{kW}{m^2}$. To withstand this temperature, inner wounded coil is made of copper tubes with 14 turns along the cavity height (coils were designed by using SWEEP function form AUTOCAD 2022 3D). As the heat source is the Sun, which is an intermittent heat source, copper was chosen for the inner tubes as it allows a quick heat transfer. This is possible since the high thermal conductivity of copper. Another advantage of copper is the price that is much lower than some other materials that could be used.

To increase the absorptivity of the received solar radiation of the wounded copper tubes, and decrease its emittance, the black chrome (Cr-Cr_2O_3) coating was supposed to be applied to the chrome tube. The black chrome coating has an emissivity of 0.09 and absorptivity of 0.84. [38]

The external casing is supposed to be made of AISI 310 stainless steel whose main characteristics are reported in the table 3. AISI 310 is a high chromium nickel austenitic stainless steel with high carbon content. It has a good resistance to heat and much lower thermal conductivity if compared to copper. [39]

Table 3 - AISI 310 main characteristics

Physical propriety	**Unit**	**Value**
Density	$\boldsymbol{kg/m^3}$	**7900**
Thermal conductivity	$W/(mK)$	23.7
Heat capacity at Constant pressure	J/(kgK)	610

Table 4 - Copper main characteristics

Physical propriety	**Unit**	**Value**
Density	$\boldsymbol{kg/m^3}$	**8960**
Thermal conductivity	$W/(mK)$	386
Heat capacity at Constant pressure	J/(kgK)	0,38

4.3 Domestic hot water storage tank sizing

Thermal demand for domestic hot water can be expressed by following equation:

$$Q_{DHW} = \dot{m} \cdot c_p \cdot (T_{use} - T_{mains})$$

Where, $\dot{m}$ is the daily demand of DHW in $\frac{kg}{person}$ and it depends on people lifestyle. For Italy this vale is assumed to be 50 $\frac{l}{person \cdot day}$. Use temperature, T_{use}, can be generally assumed to be in the rage 40÷50 °C. While the temperature from the aqueduct is related to the average temperature of the ground at 1÷2 m depth. In Italy T_{mains} will vary between 12÷14 °C in the Po Valley. Finally, assuming a home with four people, the demand for DHW is equal to around 27000 $\frac{kJ}{day}$ or 7.5 $\frac{kWh}{day}$.

To meet the demand of DHW by residential building occupied by four people, water sensible TES will be used. The range of available water TES tank is very wide, starting from small volumes up to more than 10000 L. Larger storage tanks are typically used in seasonal storage applications or for large multi – unit residential buildings. An important aspect related to the performance of a TES is maintaining a high degree of stratification. Thermal stratification allows a limited operation of the auxiliary energy supply. Stratification improves the efficiency of water tank and of the whole system too. On the other hand, storage capacity is a process variable that depends strongly on the operating condition given by the application. For sensible TES the lower and upper temperature limits determine the maximum storage capacity. However, maximum storage capacities are not accessible in real storage systems. [33]

Dimensioning of storage is based on autonomy required:

$$V = \frac{Q}{\rho \cdot c_p \cdot (T_{max} - T_{min})}$$

Where Q is the energy demand (based on number of persons and required autonomy), T_{max} is the maximum temperature in the tank (80 – 85°C for non-pressurized water tank), T_{min} is the minimum temperature for satisfying the demand (45 – 55°C). [40] By setting maximum tank temperature to 80°C (to prevent legionella disease) and minimum to 45°C and using the DHW daily demand previously calculated, a volume of 190 l is sufficient.

Energy demand for heating 190 l water tank can be evaluated by following equation:

$$E = m \cdot c_p \cdot \Delta T$$

Where:

- E is the amount of energy demand to heat up water
- $m = 190\ kg$ – water tank dimensions

- $c_p = 4185\ \frac{J}{kgK}$ – water constant
- $\Delta T = 50 - 15 = 35\,K - 50$ °C is the use temperature while 15 °C is the mains temperature.

$$E = 190 \cdot 1{,}16 \cdot 10^{-3} \cdot 35 = 7{,}71\ kWh$$

To heat up the water tank in one hour 7,71 kW are needed. Hereby presented system requires around 5 hours of irradiation as the average heat source inside the receiver is 7,45 $\frac{kW}{m^2}$ and the receiver has 0,207 m^2 surface.

5 LIFE CYCLE ASSESSMENT

5.1 LCA Introduction

Life cycle thinking has provided conceptual basis and tools to support transition to a green economy. These approaches have been developed to support the decision-making process at all levels regarding product development, production, procurement, and final disposal. Any activity or process causes environmental impacts, consumes resources, emits substances into the environment, and can generate environmental modifications throughout its life. So, life cycle assessment addresses environmental impacts of the system under study in the areas of ecological health, human health, and resource depletion. [41]

The studies of environmental impact of products started in 1960s and 1970s. At the very beginning the goal was to compare different products and it has mainly marketing purposes. The first environmental analyses were done in the USA in the 1960s and they were called REPA – Resources and Environmental Profile Analysis with focus on raw materials. In these years scientists started to change their way of thinking about optimization. Up to 1960s the processes were optimized from the point of view of one single component, supposing that increased efficiency of one unit could bring benefit to the whole system. However, this was not always the case.

One of the first studies was done by Midwest Research Institute (MRI) for Coca Cola Company in the 1969. The aim of the analysis was to define which material between glass, plastic, and aluminium was most efficient, from ecological and energy point of view, to contain Coca Cola.

In the 1970s, to the material analysis, were added also the energy analysis of the products, not only in the USA but also in Europe. This phenomenon was driven by energy crisis. At the beginning of 1990s, to the previous analysis on materials and energy was also introduced the analysis on environmental toxicology and chemistry – Framework SETAC. In the 1990s the way to conduct all the environmental analysis become standardized under ISO.

The results of global cooperation are contained in the publication “Guidelines for a Life Cycle Assessment: A code of Practice” – Society of Environmental Toxicology and Chemistry (SETAC). It contains the guidelines to use to make this kind of analysis. In the following years SETAC continued to standardize the procedures and it was followed by the International Organization for Standardization (ISO).

Following public awareness about out impact on the environment in 2006 European Commission commissioned the “Co-ordination Action for innovation in Life Cycle Analysis for Sustainability (CALCAS)”. The obtained work put in evidence the unresolved questions about suitability and the necessity of new programs and research in the future. [42]

Life cycle assessment analysis could be used as a tool to increase the awareness of producers and customers about the environmental impact and resource used. From the point of view of producer life cycle assessment of product could be: [43]

- used to make comparisons between products and materials to find the most convenient solution.
- Analyse the production processes to find the least impacting with the goal of reduction of emissions and wastes.
- Increase the competitiveness on the market and have more trust from customers.

On the other hand, from the point of view of institutions, life cycle analysis is used to:

- Labelling of products – like ecolabel
- Analyse the impacts of products with the goal to change and update the norms
- Inform the customers with the life cycle of the products they are buying.

5.2 LCA standardization

The LCA methodology is standardized by ISO 14040 and ISO 14044. ISO 14040 is the clear overview on the procedures, applications, and limitations of LCA to a spectrum of potential users and stakeholders, to help understand the meaning of life cycle assessment procedure. On the other hand, ISO 14044 is the operative one that is needed for the preparation, drafting and critical review of the inventory analysis, impact analysis phase and the phase of result interpretation. ISO/TC 207 *Environmental management* is the commission that publishes and updates the guidelines. The guidelines are reviewed by the European Committee for Standardization CEN/CS with the aim to be approved as the European norm. First versions of ISO norms about LCA were published at the end of 1990s and they are periodically updated. In particular:

- EN ISO 14040:1997: Environmental management – Life cycle assessment – Principles and framework. This norm provides the general methodology for the life cycle assessment approach. It puts in evidence objective, structure, potential, and limitations. It is not detailed technical description of LCA procedure. [44]
- EN ISO 14041:1998: Environmental management – Life cycle assessment – Goal and scope definition and inventory analysis.
- EN ISO 14042:2000: Environmental management – Life cycle assessment – Life cycle impact assessment.
- EN ISO 14042:2000: Environmental management – Life cycle assessment – Life cycle interpretation.
- EN ISO 14044: 2006: Environmental management – Life cycle assessment – Requirements and guidelines.

Version of ISO from 2006 become the landmark for the life cycle analysis.

5.3 Phases in the LCA analysis

The ISO 14040:1997 provides the definitions about product, product system, process unit and input/output:

- Product: the chosen product of analysis
- Product system: set of process units, that are connected by material and energy, which has one or more defined functions.
- Process unit: is the smallest element considered in the life cycle inventory analysis for with input and output data are quantified. The boundary of a unit process is determined by the degree of modelling detail to satisfy the purpose of the study.
- Input and output: inputs are usually raw materials and energy resources while the outputs are emissions and wastes to the environment.

From the LCA point of view, it has been seen that a "system" is defined as any set of devices that carry out one or more precise industrial operations having a specific function; it is delimited by appropriate physical boundaries with respect to the ambient system and with this it has characterized exchange relationships from a series of inputs and outputs. [45]

Moreover, when we are considering environmental impact of the product system it is important to specify that the environment it earthing that is outside the boundaries of the system. So, product system interacts with the environment or with other product systems.

A product life cycle can begin with the extraction of raw materials from natural resources in the ground and the energy generation. Materials and energy are then part of production, packaging, distribution, use, maintenance, and recycling, reuse, recovery of final disposal. In each life cycle stage, there is the potential to reduce resource consumption and improve the performance of products. [46]

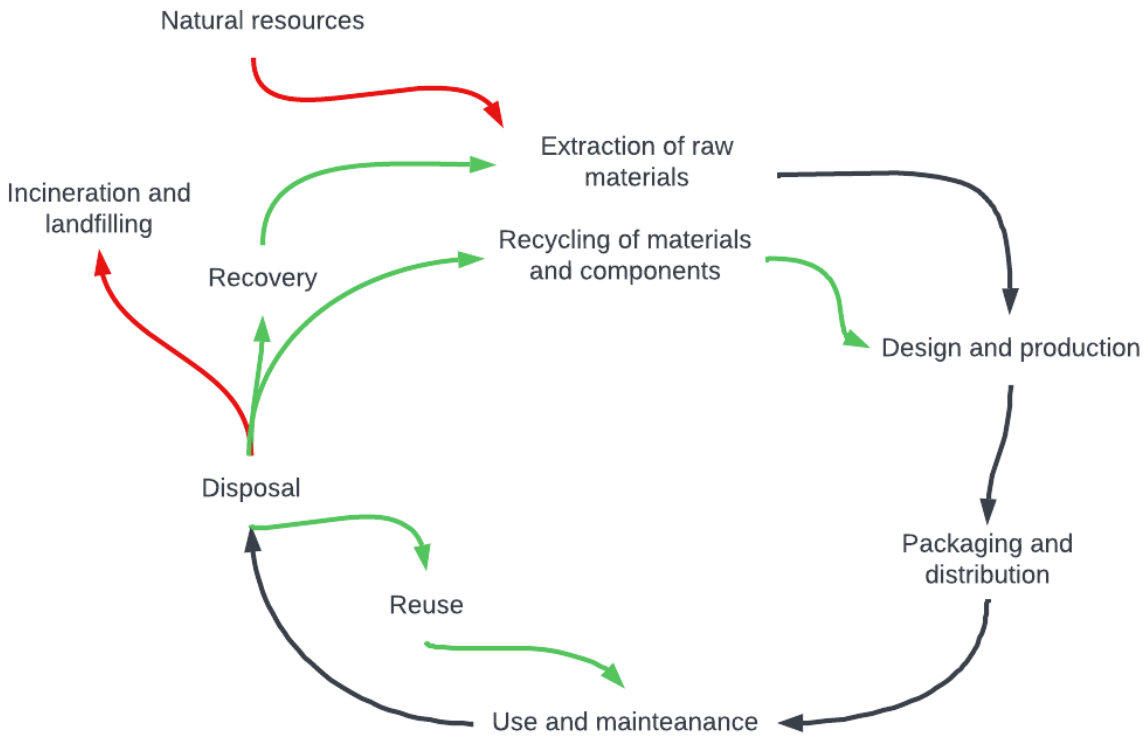

Figure 26 – Product life cycle diagram

LCA is an objective procedure, and it is used to evaluate the energy and environmental burdens related to a process or to an activity. As the analysis is objective, all assumptions must be declared to assure the transparency of the procedure.

Life cycle of a product can start with the extraction of raw materials from natural resources. This part of the analysis can include, for example, metals, water, or also ground occupation. These procedures require energy so, materials and energy used in this part will be part of all following phases. Design and production phase is the one in which the resources should be used in a rational and sustainable way. Packaging and distribution is the phase that takes

into account the delivery of the product. Use and maintenance is the part that takes place at the costumer side who is impacting on the overall environmental impact of the product. At the end life of the product different scenarios are possible:

- Disposal – leave the product without any reuse
- Incineration and landfilling – use the thermal content of the product
- Recovery – possibility to recycle parts of the product
- Reuse – reuse the product as it is

An LCA study consists of four phases:

1. Goal and scope definition of the life cycle assessment.
2. Inventory analysis that gives a description of material and energy flows within the product system and especially its interaction with environment, consumed raw materials, and emissions to the environment.
3. Impact assessments are obtained from the detailed inventory, and it is traduced in indicators. The indicator results of all impact categories are detailed in this step.
4. Interpretation of a life cycle.

In the following figure is represented the ISO 14040 guideline.

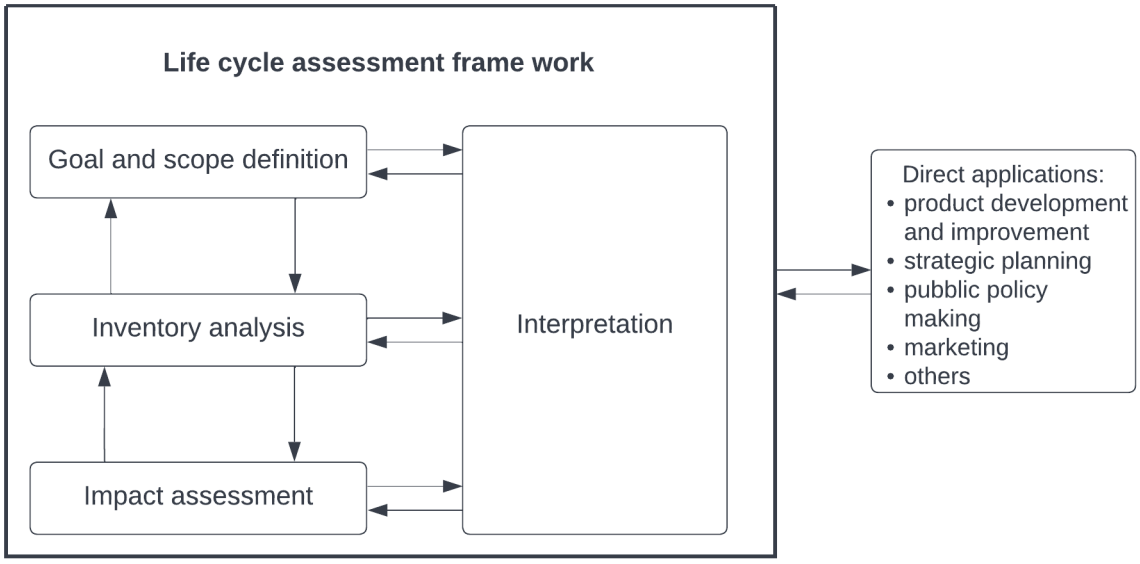

Figure 27 - ISO 14040 guideline

5.4 Definition of goal and scope

First macro phase of LCA analysis comprehends the definition of goal and scope. This phase includes following steps:

- Objective of the study: this phase defines the reasons why the LCA is done including the intended use of results. It also describes the system under analysis.

- Functional unit definition: functional unit is an arbitrary parameter used to describe the results. The functional unit must be consistent with the purpose and scope of the study. One of the main purposes of a functional unit is to provide a reference to which the data input and output are normalized, in the mathematical sense.
- System boundaries: it defines the unit processes to be included in the model. Ideally, the product system should be modelled so that the flows into and out of its boundaries are elementary flows.
- Categories of data: data can be primary, secondary, calculated or estimated for the study.
- Criteria for the inclusion of input and output: explanation of criteria about mass, energy, environment or economic used for the selection of input and output fluxes.
- Requirements for data quality: data quality is quantified by the following parameters: consistency, representativeness, reproducibility, geography, technology.

5.5 Inventory analysis

After the definition of goal and scope it is necessary to proceed with the development of inventory. The inventory analysis provides the quantification of materials and energy in input and output and their organization in a model for a given system/product. To define the inventory in a complete way the following steps must be followed:

- Flowchart: graphical representation of the system considering its boundaries
- Data procurement: procurement of data about every process unit included in the system boundaries. Data can be obtained from the manufacturer's (primary data), from literature (secondary data), from database (like Ecoinvent) or from measurements or estimates done by the person doing the analysis.
- Allocations: it is the process of characterization of input and output flows (in terms of energy and mass) of the system, product, or service.
- Inventory analysis: all the considered flows in input and output from the process units are referred to the reference flow through the normalization to the functional unit.

5.6 LCIA – Life cycle impact assessment

The goal of this phase is the evaluation of the inventory results to understand the environmental impacts categories associated with the system under analysis. For each selected impact category, proper indicators are defined. Therefore, inputs and outputs listed in LCI results are assigned to impact categories based on expected type of impact on the environment. There are two mandatory steps in this phase of evaluations: [44]

- Classification: inventory results are assigned to the impact categories to which they contribute for most.

- Characterization: results are converted in suitable indicators that is representative of the considered impact category.

There are also three optional steps in this phase, and they are: normalization (comparison with a reference value), weighting (conversion of the results using numerical factors).

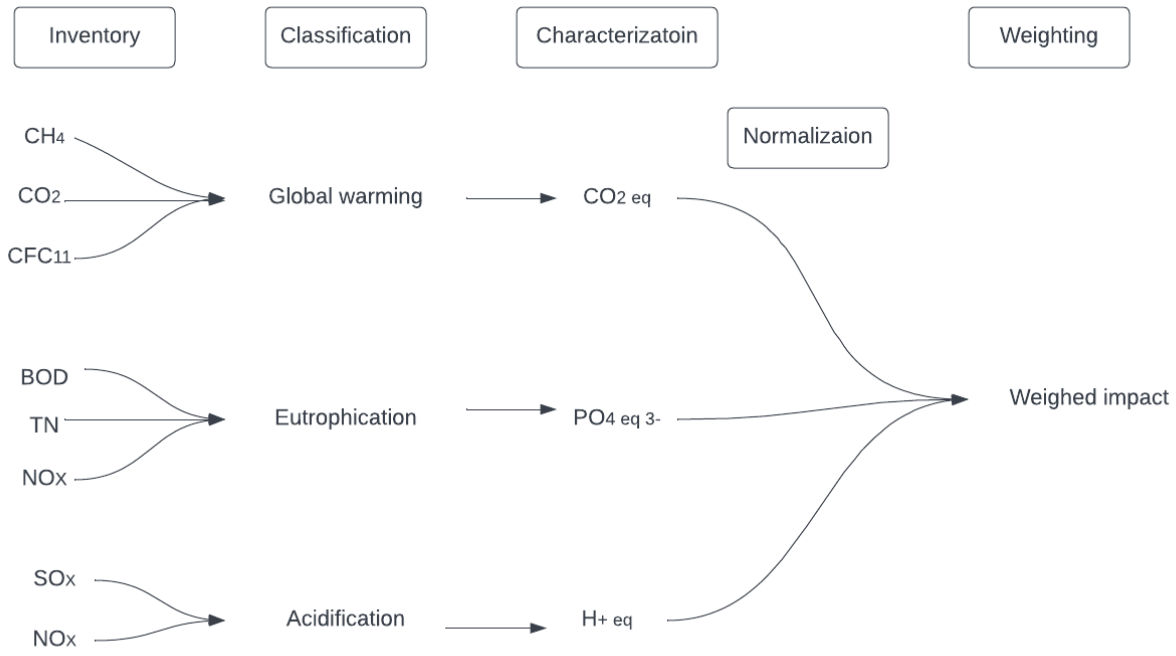

Figure 28 – Example of elements and relationships among the LCIA elements [47]

Common impact categories often considered in the LCIA are:

- Global warming
- Ozone depletion
- Acidification
- Eutrophication
- Human toxicity
- Toxicity to the ecosystem
- Toxicity to the aquatic organisms
- Consumption of materials
- Consumption of energy

Once impact categories are chosen for the study, the next step is to link the life cycle parameter to the corresponding impact category based on the cause – effect relationship. It should be noted that one parameter can affect more than one impact categories. Indeed, there are four cases where multiple impacts occur from a single inventory parameter and they are: parallel impacts (when a single inventory parameter causes more than two distinctively different impacts), serial impacts (when one inventory parameter causes two or more different types of impact in series), indirect impacts (when the negative effect is induced by inventory parameter but not caused by parameter itself), and combined impacts (when emissions of substances have a mutual influence on each other's impact). [47]

Also, the impact categories cause the effects at different scale. So, we have global (they have effect on the entire planet), regional (those that affect a large area around the impact source) and local impact (they have effect only in the area around the point of impact).

5.7 Interpretation and improvement

This is the final step of LCA in which the obtained results are used to provide guidance and recommendations on possible improvements on the investigated system. This phase can be divided in three steps:

- Identification of main issues
- Evaluation of results and they consistency
- Conclusions and recommendation.

6 LIFE CYCLE ASSESSMENT APPLIED TO PARBOLIC DISH FOR DHW PRODUCTION

6.1 Aim and Scope

Despite the big deployment of concentrating solar power plants, their environmental evaluation is still a pending issue. Reviewing literature studies about CSP LCA it can be noted that most of the references are about CSP plants based on parabolic-trough and solar tower technology. [48] Chr. Leamnatou and D. Chemisana, in their publication about LCA of concentrating systems states that CSP plant's impact depends on the water use and materials used for storage. [49] Carnevale et al. [50] presented a general case regarding the LCA of solar energy systems. Reviewing literature, it could be noted that there is need for more investigations about dish systems, storage materials, strategies for water saving, soling effect, small scale domestic systems etc. The life cycle analysis represents a fundamental tool to quantify the impacts of a product or process this, should lead to a reasonable choices that are in line with the results of the life cycle analysis.

The aim of this analysis is to study impacts of solar parabolic dish (CSP) used for the domestic hot water production (DHW) from cradle to grave, as in literature there are not present any similar studies. This might be since the deployment of this technology is still limited, not only for domestic but also at industrial scale.

LCA analysis is done on macro components of the system. These components are solar parabolic dish, solar receiver, water storage tank and pipes. This choice is due to several limitations - one of which is used database. Since the database has limited sources and since the lack of data in literature, electronics is excluded from the analysis – same is valid for welding of pieces.

Functional unit chosen in this study is "one tank of domestic hot water", and in accordance with ISO 14040 and 14044 standards, the results of the LCA are expressed in terms of this functional unit.

6.2 System Boundary

The ultimate system boundary is between the technological system and nature. In ideal case, all the inputs and outputs necessary for generation of a functional unit chosen should be followed upstream and downstream to flows of energy or matter. In other words, from nature to the technological system and from the technological system to the nature. However, if all flows are followed up to their elementary flows the system would become too complex and too large to describe and evaluate. For this reason, analysed system has in input raw materials and energy while the output is represented by emissions. [51]

The system under analysis is composed of following components, considered as the most representative:

- Parabolic dish solar concentrator
- Solar receiver
- Piping
- Water tank storage

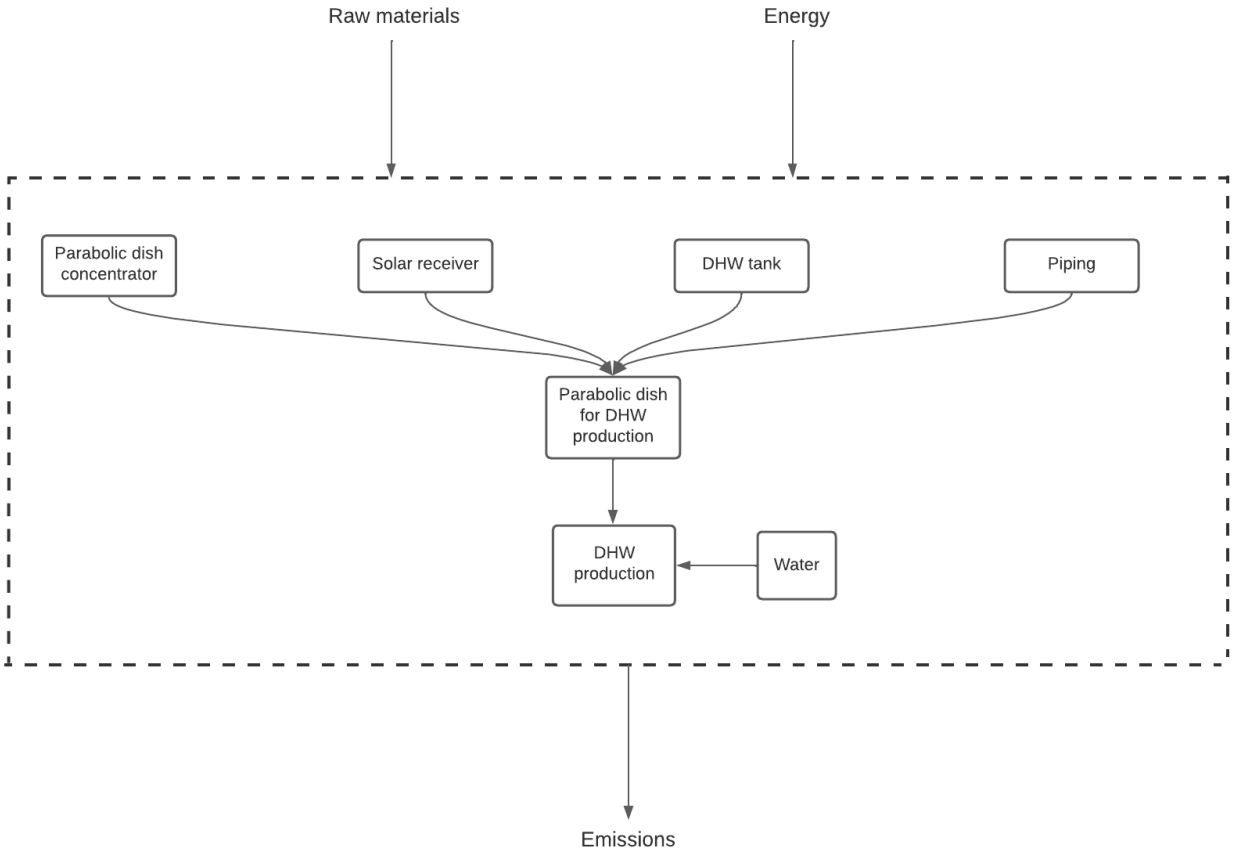

Figure 29 - Boundary system representation

The system boundary includes the phase of production, use and end life phase. To produce the system four different process of four principal systems were considered separately.

Each of the processes includes the raw materials extraction and end of life treatment. The "Parabolic dish for DHW production" process represents a process that includes all the outputs from previous processes. Indeed, it includes in input four upstream processes and their transport from the production site to the site of use.

The output of the "Parabolic dish for DHW production" process is the input for "DHW production", together with "water". The last process is represented from the functional unit to the which all results will be referred: one tank of domestic hot water.

In this last process, which is the use phase, is included also the water consumption. In this case, the transportation of water from the extraction source to the point of use is not considered

6.3 Assumptions and limitations

The production processes of hot water tank, receiver, piping, and solar collector does not include the impacts due to their assembly and manufacture. These impacts have been omitted due to the lack of reliable data. Furthermore, due to the difficulties in finding exact information regarding the quantities of used materials, it was decided to search the weight of some objects and the main materials that constitute them on the websites of retailers while some data are obtained from literature or manufacturers.

Electronic part of the system is not included in the analysis. This choice is a consequence of leak of available data. Also, some electronic components have a negligible weight if compared to other components and their overall contribution to the emissions is also negligible.

Life expectancy of the components is assumed to be equal to 30 years. Supposing to consume one full tank of water each day it can be translated in 10950 days. Assuming that the tank operates for 255 days of year and taking into account previously introduced functional unit – *one tank of domestic hot water* – weight of one day of operation is equal to 1,307E-4 of the lifespan.

6.4 Data categories and software

The data necessary to carry out LCA can be of three types:

- Primary: data obtained from documents or questionaries
- Secondary: data from literature from previously done studies or data available inside the database
- Data that are coming from personal estimations.

As the parabolic dish under analysis is in Turin, Italy, whenever it was possible, the processes used for data representation were in Italy, in Europe or in a European nation. The used software is openLCA 1.10.3 and the database is the open-source database Environmental Footprint version 1.00.

6.5 Inventory

The phase of definition of goal and scope and field of application of the study represents the starting point to conduct the second phase of the life cycle assessment which is the compilation and inventory analysis. Each unit included in the system boundaries needs to have inputs and outputs that put it in the relation with other units to create an interconnected system. The phase of Life Cycle Inventory (LCI) requires data acquisition, eventual allocations, and inventory compilation. Inventory is the list of all resources and raw

materials that enter the system and all emissions that exits the system in the amount that allow to refer it to the functional unit.

In the following imagine is graphically represented the system under analysis through the flowchart.

Figure 30 – Flowchart of the system

WATER TANK

In the system under consideration the water storage tank is a 190 l tank. The volume selected comes from the estimations done in the first part of the work.

Water storage tanks, whether used for domestic, commercial, or industrial applications, have specific requirements when it comes to their need to handle pressure, maintaining temperature, handling the corrosion and be not hazardous for human health. So, the materials that are used in their construction must respect those requirements.

Investigating on what is available as commercial offer and what is available in literature, it can be concluded that the materials, and therefore their associated proprieties, are different from tank to tank, regards on how they are intended to be used, to the components that make tank up and, who is manufacturing them.

However, it can be noted that most of the storage water tank vessels are usually made of steel alloys. As with any steel structure, corrosion is an ever-present concern. The effects of corrosion on storage tanks include premature failures and disruptions in service during repairs. The corrosion protection is obtained by glazed boilers or by cathodic protection. Anode can provide a cathodic protection against corrosion of the inner surface of tanks by means of an impressed current produced by the device. Usually both methos are used. Cathodic protection provides electrical current to the not insulated area from the environment and stops the corrosion cycle.

For this study, commercial technical sheet from EMMETI water storage tank was used for most of the data. Geometrical dimensions are: 1215 mm of height and 500 mm of diameter. In their commercial tanks, corrosion cathodic protection is done by galvanic system. This means that system relies on anodes made of metals which are more electronegative than steel: zinc and magnesium are common anode materials used for this purpose. Anode can be suspended, hanged, or attached to the tank for internal protection. [52]

Figure 31 - Magnesium anode [53]

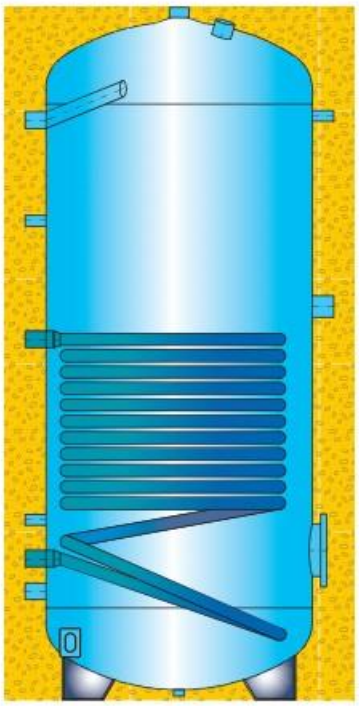

Figure 32 - Example of storage water tank with internal coil for heat exchange. Yellow part represents insulation material. [54]

Vessel of this commercial storage tank is made of carbon steel S235 JR however, this material is not present in used data base so, as alternative was chosen cold rolled, stainless steel.

Another crucial component of water storage tank is the heat exchanger. Inner heat exchanger is used to transfer heat from heat transfer fluid (HTF) to the working fluid. In this case also, several configurations are possible depending on number of coils, their position int the tank and used materials.

Her used heat exchanger is liquid – to – liquid. HTF circulates through the solar receiver, absorbs heat, and then flows through a heat exchanger to transfer its heat to potable water in the tank. The type of the heat exchanger usually used, for this kind of applications, is the coil – in – tank heat exchanger. As represented in Figure 30, coil – in – tank heat exchanger is a coil of tubing in the storage tank. For this application it is assumed that the heat exchanger, is made of two tubes – double wall heat exchanger – to prevent any kind of leakages in the potable water.

When designing a heat exchanger two most considered materials are copper and aluminium. The first one is more conductive and more costly while the second one more flexible, lighter, and cheaper. As the predicted use of the system hereby analysed is the residential sector, it was assumed that cost will be one of the points of concern. For this reason, heat exchanger made of aluminium is assumed. The surface of heat exchanger is equal to 3 m^2. This size was selected from the EMMETI technical data sheet for a 190 l water storage tank.

To keep the inside water temperature and to avoid heat loss tank must be surrounded by high performing insulating material. According to the Italian law, comma 7 of article 5 DPR 412/93, the insulation materials must be free of CFC and HCFC. For this reason, the selected

insulation material is rigid expanded polyurethane thickness 50 mm, data obtained from EMMETI technical data sheet.

As last considered part of the water storage tank is the external paint. It is assumed that paint thickness is equal to 0,2 mm [55] of alkyd paint with density equal to 1,3 kg/l [56].

The energy required for components to be assembled is not included in the analysis since there are not any data available.

MATERIAL	Unit	Value	
Stainless steel	$\boldsymbol{kg}$	**104,75**	Value estimated from technical sheet as empty weight is 120 kg.
Aluminium	kg	4,4	Value estimated considering aluminium density, heat exchanger surface and thickness
Magnesium	kg	0,5	Value found in literature
Rigid expanded polyurethane	kg	8,3	Value estimated considering data from technical specifications of water storage tank
PVC	kg	1	Estimated weight of plastics
Alkyd paint	kg	1,05	Value estimated considering the water storage geometry, paint density and its thickness.

Table 5 - Hot wate tank materials

PIPING

Hereby are included pipes that allow water flow from the receiver to the tank. It is supposed that hot water storage tank is placed at 2 meters from the tank and that pipes are made of polypropylene reinforced with fibre glass, with external thermal insulation to reduce heat losses, obtained with use of polyurethane. The data and technical details are obtained from a commercial sheet. [57]

MATERIAL	Unit	Value	
Polypropylene	***kg***	**1,13**	Value estimated from technical sheet
Polyurethane	**kg**	**1,45**	Value estimated from technical sheet

Table 6 - Piping system materials

SOLAR RECEIVER

Solar receiver is the component that was modelled in the first part of the thesis. The goal of the receiver is to heat up the working fluid.

In the past years cavity receiver has increased the allowable incident heat flux and, consequently, the operating temperature even to 1350 – 1500 K. [58] Usually, cavity receiver has five geometry types: cylindrical, conical, elliptic, spherical, and hetero – conical. Among these five types of cavity receiver, cylindrical cavity receiver is one mostly used due to the lower manufacturing cost. The heat transfer surface of the cylindrical cavity receiver is made by coiled metal tube – copper in this specific case.

Inside the coiled tubes flows heat transfer fluid with the aim of transferring the highly concentrated sun power to the working fluid. So, the heat transfer is indirect as it is firstly absorbed by the opaque solid and only then is transferred to the HTF. Therefore, the temperature is limited by the solid absorber while the heat extraction is limited by the HTF that is flowing in the receiver. HTF must be able to operate in the required temperature range, easily receive and transfer heat, and circulate well in a confined space. Main characteristics that HTF must have are [59]:

- Wide working temperature range and high thermal stability.
- High thermal conductivity of HTF is desired to enhance the heat transfer coefficient. Low viscosity is useful to reduce the pumping power.
- Low working pressure is useful to use thin tube walls. Thin walls reduce the wall temperature gradient and the temperature induced mechanical stress.
- Low hazard proprieties in terms of corrosion and safety.

Hereby presented system is thought to be used as the source of domestic hot water. The temperature that should be available at the user side is 45 °C. Usually investigated and used HTF's for solar dish systems are air, water, or thermal oil. [60]

For this application *Thermia Oil B* was chosen which is based on highly refined mineral oils from crude petroleum oil. This oil can be used in high temperature range. Some of the advantages are high thermal stability, good solvency, low viscosity, high heat transfer coefficient, and non – corrosive, low vapor pressure, non – toxic oil. [61]

Considering the heat transfer tubes, 20 l of HTF are needed for this application.

To reduce the cavity heat losses, it is supposed that cavity receiver is insulated by mineral wool insulation material. It is supposed to have 20 mm thick coating of glass wool around the receiver.

MATERIAL	Unit	Value	
Copper	kg	**11,2**	Value estimated from receiver geometry considering copper density equal to 8960 kg/m^3 [62]
AISI 310	**kg**	**21,14**	Value estimated from receiver geometry considering AISI 310 density equal to 7900 kg/m^3 [63]
Glass wool	**kg**	**0,122**	Value estimated from receiver geometry considering wool density equal to 20 kg/m^3 [64]
Thermal Oil	**kg**	**17,36**	Value estimated considering thermal oil density equal to 868 kg/m^3 [65]

Table 7 – Solar receiver materials

PARABOLIC DISH

Geometrical parameters of parabolic dish used in the first part of work are those of one available in Energy Center at Politecnico di Torino. However, it was not possible to obtain primary data about all the construction material used so, it was necessary to investigate the literature and make some assumptions.

Solar parabolic dish manufacturing and design is treated by many researchers. Publications are usually related to electricity generation, cooking, water heating and water desalination. Recommendations on material use as the geometrical parameters are also treated in several publications.

Consulting the literature on materials used for solar parabolic dish construction, *Ali Base et al., 2021* [66], in publication about the experimental design of solar parabolic receiver for water heating, used galvanized steel as construction material for solar parabolic dish and segment that holds the dish, which is covered with silver glass mirrors. However, in another experimental study, done by *Ibrahim Ladan Mohammed* [67], aluminium was used as construction material for the solar dish body which was covered by 2 mm mirror thickness to increase the reflectance.

For the LCA of this study aluminium is chosen as construction material for solar dish because of its lower weight while, the supporting structure is assumed to be made of stainless steel. It is assumed that there are 2 mm of glass thickness over a dish.

Parabolic dish available at Energy Center is equipped with tracking mechanism too. For this component data about its construction support and used materials are available directly

from the manufacturer. The used material is Fe360 structural steel. As there are not any indications about the electronic part of tracking mechanism some literature review was done.

Ibrahim L. Mohammed [67] in his experimental study used an automatic linear actuator as the tracking system. *B.E. Taranzona – Romero et al., 2021* [68] in their publication about solar tracking system used Arduino UNO chipboard. The same chipboard is used in another experimental research done by *Asif Ahmet et al., 2020*, [69]. Assuming to have electronic part of the system made by Arduino UNO, as its complete weight is around 250 g, compared with other materials quantities, this can be neglected – as previously assumed.

MATERIAL	Unit	Value	
Stainless steel	$\boldsymbol{kg}$	**592,5**	Value calculated considering the available design of parabolic dish structure with stainless steel density equal to 8000 kg/m^3. [70]
Aluminium	**kg**	**320**	Value estimated through calculation of collector area and its thickness, considering aluminium density equal to 2710 kg/m^3. [71]
Glass	**kg**	**20**	Value estimated through calculation of collector area, with 2 mm of glass thickness, considering glass density equal to 2500 kg/m^3. [72]
Structural steel	**kg**	**0,9**	Value calculated considering the available design of solar tracking system, considering structural steel density equal to 7850 kg/m^3 [73]

Table 8 - Parabolic dish materials

END OF LIFE

End-of-life treatment in OpenLCA software is possible through flows called “waste”. These flows must be inserted in the output of the process.

The used methodology to the end-of-life treatment is the so-called Cut-off method. With this method, model terminate with the waste collection and treatment, excluding the phase of recycling and of realization of new product. [74]

End of life treatment was applied to copper, glass wool, stainless steel, hot water tank and aluminium. For some of the materials it was not possible to model the end-of-life since the used database is very limited and there were not any proxies about its treatment.

USE PHASE

Final process is the “System Use” whose reference is the production of one tank of hot water. It was assumed that the hole system can operate for 30 years. It was assumed that the system for water production would be used every day and supposing to be able to produce one tank of hot water (190 l) for 255 days of 365 days in the year or 69,86 % of the days in a year.

The lifetime of the system can be translated in 10950 days or in 7650 operational days. So, the production of one tank of hot water contributes by 1.30719E-4.

Inputs to the use phase are all previously described process, including transportation, and 190 l of water. It is assumed that the whole system is fabricated 500 km away from the location of use and then transported on road with articulated lorry transport.

Manutention of the system is not considering because of leak of data on the subject.

In conclusion, in the use of the system are included: production of solar collector, production of solar receiver, production piping system, production of hot water tank storage, transportation from the fabrication place to the use phase, the use of the system and life end of pieces.

6.5.1 Allocation

ISO 14044:2006 suggest avoiding the allocation phase whenever possible. In the modelled processes the allocation is not needed as co products are not obtained. For this reason, in the OpenLCA modelling software no allocation was chosen.

6.5.2 Results from the inventory analysis

Once the main materials were included in the process of components production, product system was created. Then, Environmental Footprint (Mid-point indicator) was chosen as the impact assessment method, because of used database Product Environmental Footprint.

Mid-point method is based on cause-effect chain between resource consumption/emissions and the endpoint level. This method is used to obtain indicators for environmental impact comparisons. [75]

Obtained inventory contains all the input and output components that include entire lifetime of each modelled product. The inventory is composed of fluxes that are exchanged between system and the environment. Input is characterized by the consumed resources in terms of raw materials, energy, or land use while in output are present emissions in air, in water or in land. Since the list of inputs and outputs is huge it was chosen to use the cut off value equal to 1%. In this way 297 input components were obtained and 1890 output components. In the Attachment 1 is provided the list of first 100 input components, referred to the functional unit and in decreasing order while the Attachment 2 contains emissions. In the following Table 9 are reported first twenty input quantities, in decreasing order:

Input				
Flow	**Category**	**Sub-category**	**Unit**	**Result**
hard coal	Resources	From ground	MJ	3.9E+00
inert rock	Resources	From ground	kg	3.9E+00
Water (rain water)	Resources	From water	kg	2.8E+00
Air	Resource	in air	kg	2.5E+00
natural gas	Resources	From ground	MJ	2.1E+00
crude oil	Resources	From ground	MJ	1.5E+00
sea water	Resources	From water	kg	1.5E+00
primary energy from hydro power	Resources	From water	MJ	7.5E-01
primary energy from solar energy	Resources	From air	MJ	3.0E-01
Uranium	Resource	in ground	MJ	2.7E-01
brown coal	Resources	From ground	MJ	2.4E-01
primary energy from geothermics	Resources	From ground	MJ	2.4E-01
Water to turbine	Resources	From water	m3	1.6E-01
Iron	Resource	in ground	kg	1.1E-01
primary energy from wind power	Resources	From air	MJ	1.1E-01
Silicon	Resource	in ground	kg	7.6E-02
Magnesium	Resource	in ground	kg	6.9E-02
Aluminium ingot	Materials production	Metals and semimetals	kg	4.3E-02
calcium carbonate	Resources	From ground	kg	2.8E-02
carbon dioxide (biogenic)	Resources	From air	kg	2.3E-02

Table 9 – Inputs obtained from inventory analysis and referred to the functional unit of the system

Between the mostly used materials there are hard coal, inert rock, water, natural gas, and crude oil. These materials are linked to the extraction and manufacturing processes of materials. On the other hand, the other forms of renewable energy could be linked to the electricity consumption during fabrication phase.

For what concern the emission flows same reasoning is done. Since the number of output flows is big in the following table are reported mostly polluting sources which are emitted in air and/or in water.

Emissions				
Flow	**Category**	**Sub-category**	**Unit**	**Result**
carbon dioxide (fossil)	Emissions	Emissions to air	kg	6.51E-01
carbon dioxide (biogenic)	Emissions	Emissions to air	kg	2.26E-02
sulfur dioxide	Emissions	Emissions to air	kg	3.10E-03
nitrogen dioxide	Emissions	Emissions to air	kg	1.45E-03
carbon monoxide (fossil)	Emissions	Emissions to air	kg	1.26E-03
Nitrogen monoxide	Emissions	Emissions to air	kg	5.66E-05
nitrous oxide	Emissions	Emissions to air	kg	1.09E-05
Nitrogen oxides	Emissions	Emissions to air	kg	9.24E-06
Carbon monoxide (biogenic)	Emissions	Emissions to air	kg	1.40E-06
sulfate	Emissions	Emissions to air	kg	3.95E-07
sulfate	Emissions	Emissions to water	kg	4.14E-04
Phosphorus	Emissions	Emissions to water	kg	3.12E-07
sulfur	Emissions	Emissions to water	kg	6.44E-09
sulfur trioxide	Emissions	Emissions to water	kg	4.04E-10
sulphuric acid	Emissions	Emissions to water	kg	9.19E-11
nitrogen dioxide	Emissions	Emissions to water	kg	2.40E-11
carbon disulfide	Emissions	Emissions to water	kg	6.50E-12

Table 10 – Emissions to air and to water from main polluting elements obtained from inventory analysis and referred to the functional unit of the system.

Main polluting element is carbon dioxide, that could be due to the energy production, some is derived from fossil fuels (fossil) other part is a result of combustion or decomposition of organic materials (biogenic).

6.6 Impact evaluations of main components

Analysis of each component starts with raw materials, includes fabrication phase, transportation from the factory to the place of assembly and, end of life treatment. In the use phase water consumption was added while the manutention is not included due to lack of data.

Impact category climate change is represented with EF Impact Assessment Model – Bern model: Global Warming Potentials (GWP) over a 100-year time horizon and indicator is expressed in terms of kg CO_2 equivalent. [75] In following figures is represented climate change impact category for four modelled processes.

End of life treatment was applied only to the materials for which it was possible: copper, aluminium, steel, polyurethane, glass wool. The end – of – life treatment, as previously said, was included in the in the production process of each component.

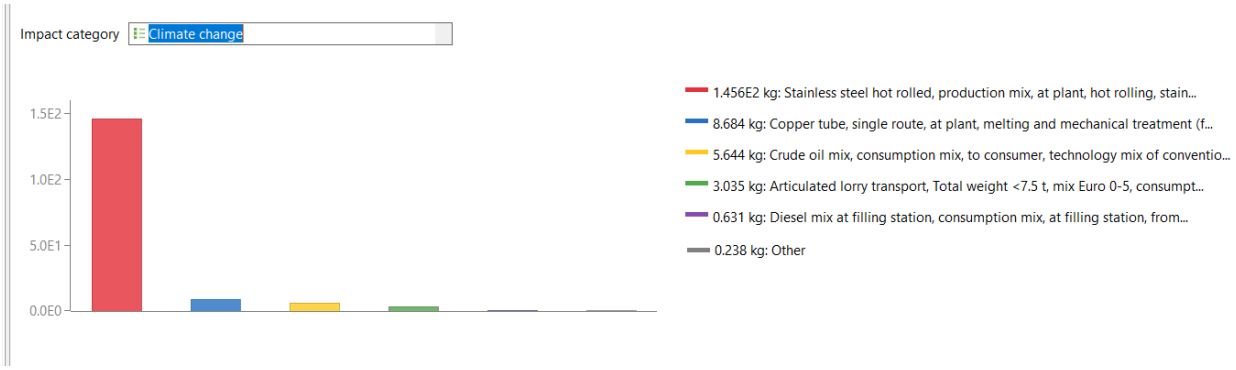

Figure 33 - Climate change impact category for cavity receiver production

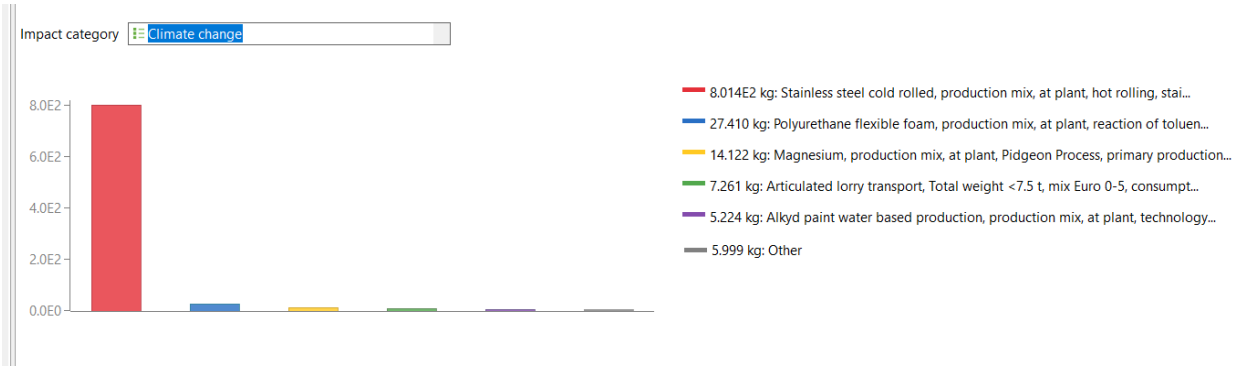

Figure 34 - Climate change impact category for hot water tank production

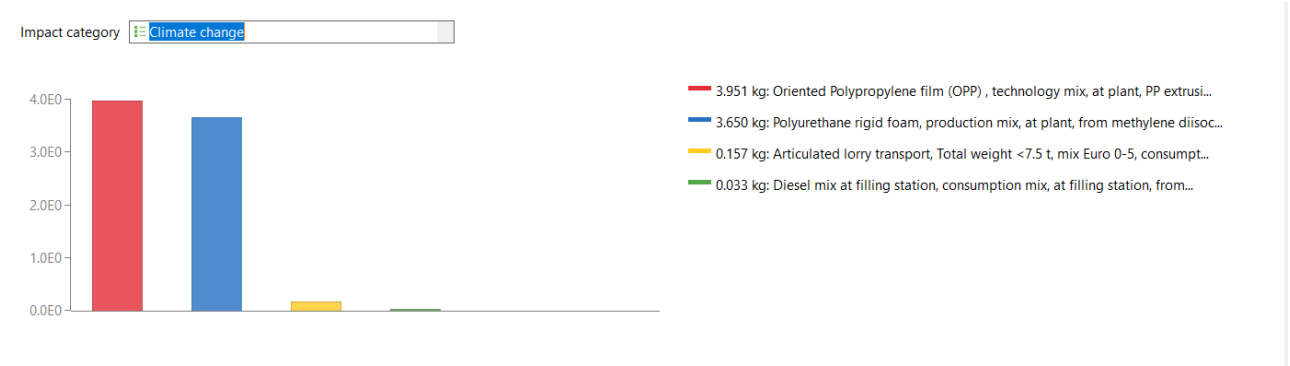

Figure 35 - Climate change impact category for piping system production

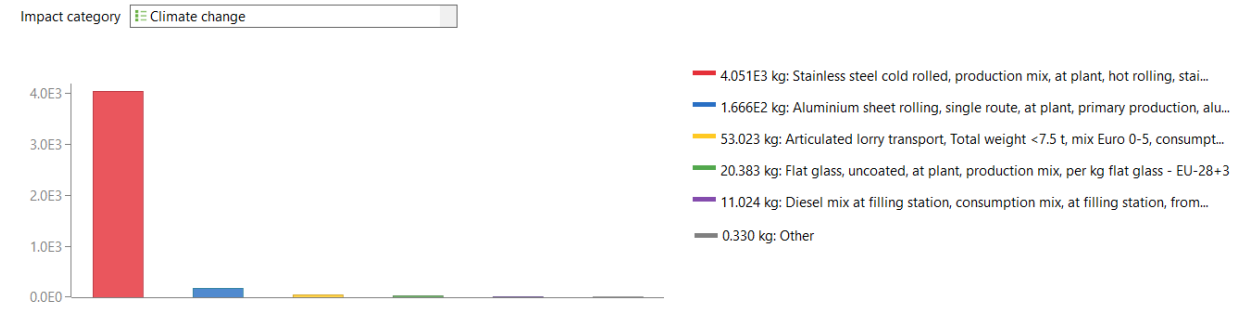

Figure 36 - Climate change impact category for parabolic dish production

In each process, except for piping tubes, stainless steel production is the biggest contributor for the climate change impact category. For both technologies of steel production, hot and cold rolled, available dataset covers all relevant steps in the supply chain while the inventory

of the process is mainly based on industrial data. The production process of steel in used dataset is based on internationally adopted production processes connected with regional precursor chains. Even if steel production is energy intensive and big emitter of GHG, steel can be completely recycled indefinite number of times. However, in this analysis was not included any recycled steel as input material.

In following table are represented major indicators for each analysed process.

Indicator	*Parabolic dish*	*Hot water tank*	*Cavity receiver*	*Piping line*	*Unit*
Acidification	32.303	6.413	1.242	0.017	mol H+ eq
Climate change	4.30E+03	8.61E+02	1.64E+02	7.79E+00	kg CO2 eq
Ecotoxicity, freshwater	2.61E+03	5.45E+02	1.05E+02	1.16E+00	CTUe
Eutrophication, freshwater	5.10E-03	1.56E-03	1.80E-04	3.62E-05	kg P eq
Human toxicity, cancer	4.90E-05	1.03E-05	2.08E-06	6.81E-08	CTUh
Human toxicity, non-cancer	1.90E-04	6.43E-05	1.35E-07	6.85E-07	CTUh
Ionising radiation, human health	7.54E+01	1.03E+01	3.02E+00	4.14E+02	kg U235 eq
Land use	5.82E+03	1.18E+03	1.97E+02	2.96E+01	
Ozone depletion	6.84E-08	3.17E-07	2.53E-09	6.67E-06	kg CFC-11 eq
Particulate matter	5.18E-04	1.04E-04	1.85E-05	1.51E-07	kg PM2.5 eq
Photochemical ozone formation	1.19E+01	2.33E+00	4.66E-01	1.40E-02	kg NMVOC eq
Resource use, fossil	4.91E+04	1.00E+04	2.58E+03	1.93E+02	MJ
Resource use, minerals, and metals	2.08E-01	4.10E-02	8.08E-06	3.52E-06	kg Sb eq
Water use	1.27E+03	2.59E+02	4.21E+01	1.42E+00	m3

Table 11 - Comparison between main components for analysed impact categories

The most impacting process in all categories, except for ozone depletion, is parabolic dish fabrication. As previously shown for the climate change only, steel is the least environmentally friendly as its fabrication is energy intensive. This assumption is valid also for other impact categories and, as parabolic dish is the element that contain major quantity of steel, it results also the biggest contributor to impact categories.

On the other hand, for the ozone depletion indicator the biggest contributor is the piping line fabrication process. This contribution is due to the use of polyurethane as insulating material. The only available dataset for this material covers its entire life cycle with inventory based on industry form Europe (EU-28+EFTA).

6.7 CO_2 emissions in case of traditional DHW boiler

Considering the previous assumption of domestic hot water consumption of a house of four people:

$$Q_{DHW} = \dot{m} \cdot c_p \cdot (T_{use} - T_{mains}) = \ 27000 \ \frac{kJ}{day} = 6453{,}15 \ \frac{kcal}{day}$$

Assuming an efficiency of DHW boiler equal to 93%:

$$Q_s = \frac{Q_{DHW}}{\eta} = 6938{,}87 \ \frac{kcal}{day}$$

Supposing that the DHW boiler is fuelled by CH_4 with a lower calorific value equal to 8550 $\frac{kcal}{m^3}$, it leads to a fuel consumption equal to 0,812 $\frac{m^3}{day}$.

Considering the stoichiometric calculations for methane combustion:

$$CH_4 + 2O_2 \rightarrow CO_2 + H_2O$$

$$22{,}4 : 22{,}4 = 1 : CO_2$$

$$CO_2 = 1 \ \frac{m_n^3}{m_n^3 \ CH_4} \rightarrow \ CO_2 = \frac{1 * 44}{22{,}4} = 1{,}96 \ \frac{kg}{m_n^3 \ CH_4}$$

It means that, for one day 1,6 kg of CO2 are emitted. Assuming the same emissions for 30 years and, considering the same number of days of operation as for solar dish, 12240 kg of CO_2 are emitted. This number results just from the operation phase of the plant and it is much larger that the one obtained from production process of four previously analysed solar parabolic dish components.

7 Conclusions

In this study a parabolic dish system for domestic hot water production was evaluated. Hereby analysed system is driven by renewable solar energy during its operation so, that phase is not characterized by any relevant polluting emissions. However, fabrication of the system requires non-renewable resources whose fabrication process leads to polluting emissions. As parabolic dish system is characterized by this who phases, the thesis was divided in two parts.

In the first part of work cavity receiver geometry was analysed with COMSOL Multiphysics software to select suitable materials for its construction. To do this parabolic dish system present in Energy Center of Politecnico di Torino was used as the input parameter. In particular, the reflector geometrical characteristics were used to model the reflector inside Ray Tracking Module COMSOL's library. To do this a comparison between ideal and real reflector was done. To model real reflector, factors such as reflector absorption, surface roughness and limb darkening were introduced. In both, ideal and real cases of solar reflector, receiver was a circular flat surface. Both conditions lead to an extremely high temperatures on receiver surfaces which in real reflector case is around 4000 K.

Second step was the receiver design. Consulting several scientific publications, cylindrical cavity receiver was chosen for this application. Main motivation behind this choice is the trade-off between its cost and efficiency. Cavity receiver is supposed to be placed at focal distance from the receiver and its radius is equal to 115 mm with 230 mm of height. To perform heat exchange between concentrated solar radiation and working fluid, inner copper tubes were designed. In this new configuration the maximum internal temperature is equal to 1146,9 K. Copper was selected as material for heat transfer tubes because of its high thermal conductivity, low cost, and good performance at high temperatures. The external envelope of cavity receiver is supposed to be made by steel AISI 310 since it can operate at high temperature but has much lower thermal conductivity if compared to copper. AISI 310 is the first barrier to heat loss in the system. To avoid additional heat losses, it is supposed that cavity receiver envelope is insulated with 20 mm of glass wool.

First part of the thesis was performed entirely on COMSOL Multiphysics software. So, the limitations encountered were mainly due to the computational capabilities of used device. Mesh selection, for example, was chosen as a compromise between accuracy and computational capability of used PC.

In the second part of thesis Life Cycle Assessment of domestic hot water production system was performed. The analysis was done with OpenLCA software with free database: Product Environmental Footprint, developed by European Commission research center.

Life Cycle Assessment was performed on four main components: solar parabolic dish, solar receiver, piping system and hot water tank. For each component selected materials are chosen in accordance with currently used in commercial offer or materials from experimental scientific publications. Particularly, for domestic hot water tank and piping system materials, technical data sheets were consulted. Materials for parabolic dish were

selected in accordance with the scientific publications while for solar receiver materials are derived from the first part of thesis.

Process that represents the entire story, from cradle to grave, was modelled for each component. In the process is included also the transportation phase from place of fabrication to the place of assembly.

Several impact categories were analysed. Most polluting material, between those selected for components, is stainless steel. These emissions could be reduced if recycled materials would be used in input.

Performed Life Cycle Assessment analysis is limited by available data in used database and by lack of informations. Since the used database is limited, some processes were mandatory to choose as they were the only option. For what concerns data availability, in LCA analysis is not included energy needed for welding nor the energy needed for pump during the use phase. Also, electronics is not included since the weight of components is low, if compared to other components.

Despite the emissions during the fabrication phase, solar parabolic dish could be used as a great alternative to the traditional domestic hot water production systems. As demonstrated with a simple stoichiometric calculation in the paragraph 6.7, the CO_2 emissions only during the operation phase, are much bigger than those obtained during the fabrication process of four analysed components together.

Technological development could reduce the costs of this systems and they could become more economically viable and even more environmental friendly.

References

[1] F. Solomone, F. Piers, G. Veronika, H. Collins, K. Haroon, K. Shigeki, K. Elmar, M. Luis, S. Roland and V. V. Maria, “Globar warming of 1.5 °C - Chapter 2: Mitigation Pathways Compatible with 1.5°C in the Context of Sustainable Development,” IPCC, 2018.

[2] E. Commission, “Energy and the Green Deal,” 2019.

[3] IEA, “Heating,” Paris, 2020.

[4] ISI, ISE, IREES, Observ'ER, EEG and TEP, “Mapping and analyses of the current and future (2020 - 2030) heating/cooling fuel deployment (fossil/renewables),” Karlsruhe, Freiburg, Paris, Vienna, Zurich, 2016.

[5] Solar Heat Europe, “http://solarheateurope.eu,” 2019. [Online]. Available: http://solarheateurope.eu/policy/heating-cooling/.

[6] IEA, “TASK 55 - Integrating Large SHC Systems into DHC Networks,” Solar Heating & Cooling Programme - International Energy Agency, 2020.

[7] M. Abid, M.S. Khan, Hussain Ratlamwala T.A., “Thermodynamic Performance Evaluation of a Solar Parabolic Dish Assisted Multigeneration System,” *Journal of Solar Energy Engineering,* vol. J. Sol. Energy Eng, no. 41(6): 061014, 2019.

[8] K. Reddy, G. Veershetty and T. S. Vikram, “Effect of wind speed and direction on convective heat losses from solar parabolic dish modified cavity receiver,” *Solar Energy,* vol. Volume 131, no. ISSN 0038-092X, pp. Pages 183 - 198, 2016.

[9] J. C. McVeigh, Sun Power: An Introduction to the Applications of Solar Energy, PERGAMON PRESS, 1983.

[10] IEA, “Electricity Information: Overview,” IEA, Paris, 2021.

[11] S. G. o. P. Luis Crespo, “HELIOSCSP SOLAR THERMAL ENERGY NEWS,” 23 01 2014. [Online]. Available: https://helioscsp.com/50-concentrated-solar-power-csp-and-2304-mw-in-spain-by-luis-crespo/. [Accessed 11 06 2022].

[12] IEA, “Technology Roadmap - Concentrating Solar Power,” Paris, 2010.

[13] SolarPACES, “www.solarpaces.org,” 2021. [Online]. Available: https://www.solarpaces.org/csp-technologies/csp-projects-around-the-world/.

[14] P. Marc and P. Richard, “A fundamental look at supply side energy reserves for the planet,” IEA, 2015.

[15] *The History of Solar,* U.S. Department of Energy.

[16] W. S. K. Lovegrove, “Introduction to concentrating solar power (CSP) technology,” in *Concentrating solar power technology - Principles, developements and applications*, Cambridge, Woodhead Pubblishing Series in Energy: Number 21, 2012, pp. 3-5.

[17] C. Meriem, V. Sèbastien and B. Tijani, “Benchmark of Concentrating Solar Power Plants: Historical, Current and Future Technical and Economic Development,” *Procedia Computer Science,* vol. 83, pp. 782-789, 2016.

[18] D. Mills, “Linear Fresenel reflector (LFR) technology,” in *Concentrating Solar Power Technology: Principles, Developements and Applications*, Australia, Woodhead Pubblishing Series in Energy: Number 21, 2012, pp. 153-156.

[19] F. Wang, Z. Cheng, J. Tan, Y. Yuan, Y. Shuai and L. Liu, “Progress in concentrated solar power technology with parabolic trough collector system: A comprehensive review,” *Renewable and Sustainable Energy Reviews,* vol. 79, no. 1364-0321, pp. 1314-1328, 2017.

[20] R. Islam, B. A. B. M. N. and U. M. W., “An overview of Concentrated Solar Power (CSP) technologies and its opportunities in Bangladesh,” International Conference on Electrical, Computer and Communication Engineering (ECCE), Cox’s Bazar, Bangladesh, 2017.

[21] Z. M. Eduardo, “Parabolic-trough concentrating solar power (CSP) system,” in *Concentrating solar power technology - Principles, developements and applications* , Woodhead Pubblishing Series in Energy: Number 21, 2012, pp. 197-198.

[22] V.-H. Lorin, “Central tower concentrating solar power (CSP) systems,” in *Concentrating solar power technology - Principles, developments and applications*, Woodhead Publishing series in Energy, 2012, pp. 240-244.

[23] Z. Eduardo, V. Loreto, L. Javier, H. Klaus, E. Markus, -D. W. H and E. Martin, “Direct steam generation in parabolic troughs: Final results and conclusions of the DISS project,” *Energy,* vol. 29, no. 0360-5442, pp. 635-644, 2004.

[24] S. Wolfgang and K. Thomas, “Parabolic dish concentrating solar power (CSP) systems,” in *Concentraing solar power technology - Principles, developments and applications*, Stuttgart, Woodhead Publishing Series in Energy, 2012, pp. 284-288.

[25] K. S. Susant, S. K. Arjun and K. N. Sendhil, “Design and developement of a low-cost solar parabolic dish concentrator system with manual dual-axis tracking,” *International Journal of Energy Research ,* vol. 45, pp. 6446-6456, 2021.

[26] P. Andreas, K. George and H. Ioannis, “Parametric analysis for the installation of solar dish technologies in Mediterranean regions,” *Renewable and Sustainable Energy Reviews,* vol. 14, pp. 2772-2783, 2010.

[27] C. Joe and A. Charles, “Dish system for CSP,” *Solar Energy,* vol. 152, no. 0038-092X, pp. 140-170, 2017.

[28] T. Vanita, D. Ankush and R. Akshaykumar, “Performance Analysis Methodology for Parabolic Dish Solar Concentrators for Process Heating Using Thermic Fluid,” *Journal of Mechanical and Civil Engineering,* vol. 12, pp. 101-114, 2015.

[29] U.S. DEPARTMENT OF ENERGY , “SOLAR TOTAL ENERGY PROJECT, SHENANDOAH - SYSTEM DESCRIPTION FINAL DESIGN REPORT,” GENERAL ELECTRIC - Advanced Energy Department, 1980.

[30] K. L. Chin, S. L. Yun and Y. K. Shin, “Improvement of bifacial solar panel efficiency using passive concentrator and reflector system,” *International Conference on Renewable Energy Research and Applications (ICRERA),* no. 10.1109/ICRERA.2013.6749723., pp. 42-45, 2013.

[31] enerMENA German Aerospace Center (DLR), “Towards a Sustainable Implementation of Solar Thermal Power Plants Technology in the MENA,” in *Renewable Energy Seminar of the Arab Union of Electricity and the EIJLLPST Project*, Amman.

[32] E. N. Jorge and C. P. José, “A comprehensive and fully predictive discrete methodology for volumetric solar receivers: application to a functional parabolic dish solar collector system,” *Applied Energy,* vol. 267, no. 114781,, 2020.

[33] L. F. Cabeza, I. Martonell, L. Mirò, A. I. Fernàndez and C. Barrenceche, Introduction to thermal energy storage (TES) systems, Cambridge, UK: Woodhead Publishing, 2015.

[34] S. Wolf-Dieter, “Thermal energy storage systems for concentrating solar power (CSP) plants,” in *Concenctrating solar power technology*, Woodhead Publishing , 2012, pp. 362-392.

[35] COMSOL Software, “Ray Optic Module User's Guide,” 2017.

[36] COMSOL Software, “Solar Dish Receiver,” [Online]. Available: https://www.google.com/url?sa=t&rct=j&q=&esrc=s&source=web&cd=&ved=2ahUKEwjy_-bFpOb1AhVb57sIHVW_D1UQFnoECAsQAQ&url=https%3A%2F%2Fwww.comsol.com%2Fmodel%2Fdownload%2F660561%2Fmodels.roptics.solar_dish_receiver.pdf&usg=AOvVaw27Vb44fgSnxRAsQoDQ9t4O.

[37] W. G. l. Roux, T. B. -. Ochende and J. P. Meyer, “Thermodynamic optimisation ofn the integrated design of a small - scale solar thermal Brayton cycle,” *International Journal of Energy Research,* vol. 36, pp. 1088-1104, 2012.

[38] R. Loni, A. -. A. E. Askari, B. Ghobadian and A. Kasaeian, “Experimental study of carbon nano tube/oil nanofluid in dish concentrator using a cylindrical cavity receiver: Outdoor tests,” *Energy Conversion and Managment ,* vol. 165, pp. 593-601, 2018.

[39] “theworldmaterial.com,” [Online]. Available: https://www.theworldmaterial.com/aisi-310-stainless-steel/. [Accessed 23 giugno 2022].

[40] S. Marco, “Solar Water Thermal System,” in *Soral Thermal Technologies Course slides*, Politecnico di Torino, 2020.

[41] V. Piemonte, P. Falco MDe Tarquini and A. Giaconia, “Life Cycle Assessment of a high temperature molten salt concentrated solar,” *Sol. Energy,* vol. 1101–1108, p. 85, 2011.

[42] J. G. e. al., “Life cycle assessment: Past, Present, and Future,” *Environ. Sci. Technol.,* vol. 45, pp. 90-96, 2011.

[43] ARCA, “Linee guida ARCA per il Life Cycle Assessment,” 2914.

[44] e. C. I. 207, “UNI EN ISO 14040:1997:,” 1997.

[45] “PeaceLink - telematica per la pace,” [Online]. Available: https://lists.peacelink.it/economia/2005/09/msg00037.html. [Accessed 19 05 2022].

[46] Life Cycle Initiative, “What is Life Cycle Thinking?”.

[47] Ministry of Commerce; Industry and Energy - Republic of Corea; Cooperation, Asia - Pacific Economic, “Life Cycle Assessment - Best practices of ISO 14040 series,” Committee on Trade and Investment, 2004.

[48] D. C. Chr. Lamnatou, “Concentrating solar system: Life Cycle Assessment (LCA) and envirnomental issues,” *Renewable and Sustanable Energy Reviews,* vol. 78, pp. 916-932, 2017.

[49] C. Lamnatou and D.Chemisana, “Concentrating solar systems: Life Cycle Assessment (LCA) and environmental issues,” *Renewable and Sustainable Energy Reviews,* vol. 78, pp. 916-932, 2017.

[50] E. Carnevale, L. Lombardi and L. Zanchi, “Life Cycle Assessment of solar energy systems: Comparison of photovoltaic and water thermal heater at domestic scale,” *Energy,* vol. 77, pp. 434-446, 2014.

[51] A. Tillman, T. Ekvall, H. Baumann and T. Rydberg, “Choice of system boundaries in life cycle assessment,” *J Clean. Prod.,* vol. 2, p. 21–29, 1994.

[52] T. Huck, “Water World,” [Online]. Available: https://www.waterworld.com/home/article/16193626/cathodic-protection-for-above-ground-storage-tanks. [Accessed 05 May 2022].

[53] “RVupgrades.com,” [Online]. Available: https://www.rvupgradestore.com/Magnesium-Anode-Rod-p/09-0205.htm. [Accessed 05 May 2022].

[54] “EMMETI Bollitori,” 2022.

[55] AMERICAN-WATER-Military-Services, “Standard Specifications Water Storage Tank Painting,” 2013.

[56] JOTUN, “Alkydprimer Technical Data Sheet,” 2021.

[57] I. 2000, “RENO PP-FIBER,” Castelnuovo Garfagnana .

[58] A. Segal and M. Epstein, “The optics of the solar tower reflector,” *Solar Energy,* vol. 69, pp. 229-241, 2000.

[59] K. Clifford and D. I. Brian, “Review of high - temperature central receiver designs for concentrating solar power,” *Renewable Sustainable Energy ,* vol. 29, pp. 835-846, 2014.

[60] P. Sasa, M. D. Ahmed, B. Evangelos, S. Velimir, S. Mahmoud and K. A.-D. Raya, “Experimental and numerical investigation on the optical and thermal performance of solar parabolic dish and corrugated spiral cavity receiver,” *Journal of Clear Production,* vol. 150, pp. 75-92, 2017.

[61] Shell, “Shell Thermia Oil B”.

[62] R. S. o. Chemistry, “rsc.org,” Royal Society of Chemistry 2022, [Online]. Available: https://www.rsc.org/periodic-table/element/29/copper. [Accessed 01 07 2022].

[63] “thyssenkrupp materials engineering.tomorrow.together,” thyssenkrupp Materials (UK) Ltd, [Online]. Available: https://www.thyssenkrupp-materials.co.uk/stainless-steel-310-14845.html. [Accessed 01 07 2022].

[64] ISOVER, “Safe Use Instruction Sheet - ISOVER glass wool,” 2016.

[65] Shell, “Shell Thermia Oil B - High performance heat trasnfer fluid,” 2009.

[66] B. Ali, M. M., H. A. Mohammed and M. E.-M. Wael, “The design of a hybrid parabolic solar dish - steam power plant: An expertimental study,” *Energy Reports,* vol. 8, pp. 1949-1965, 2022.

[67] L. M. Ibrahim, “Design and development of a parabolic dish solar water heater,” *International Journal of Engineering Research and Applications (IJERA),* vol. 2, pp. 822-830, 2012.

[68] E. T.-R. B, C.-C. A, L. S.-R. C, G. A.-V. J and D. R.-Q. A, “Design and construction of a solar tracking system for linear fresnel concentrator,” *Periodicals of Engineering and Natural Sciences,* vol. 9, pp. 778-794, 2021.

[69] A. Asif, N. A. Mohd, M. S. Dur and N. Murad, “Design of parabolic solar dish tracking system using arduino,” *Indonesian Journal of Electrical Enginnering and Computer Science ,* vol. 17, pp. 914-921, 202.

[70] D. o. Steel, “hypertextbook,” [Online]. Available: https://hypertextbook.com/facts/2004/KarenSutherland.shtml. [Accessed 03 07 2022].

[71] “thyccenkrupp,” thyssenkrupp Materials (UK) Ltd, 2022. [Online]. Available: https://www.thyssenkrupp-materials.co.uk/density-of-aluminium.html. [Accessed 03 07 2022].

[72] “saint-gobain-building-glass,” [Online]. Available: https://uk.saint-gobain-building-glass.com/en-gb/architects/physical-properties. [Accessed 03 07 2022].

[73] “geocentrix.co.uk,” [Online]. Available: https://www.geocentrix.co.uk/help/content/items/steels/fe_grade_steels.htm. [Accessed 03 07 2022].

[74] N. Andres, P. Sofia, C. Mudit, B. d. O. Felipe, T. Johan and A. Rickard, “Methodological Approaches to End-Of-Life Modelling in Life Cycle Assessments of Lithium-Ion Batteries,” *batteries,* vol. 51, 2019.

[75] E. Commission, “Indicators and targets for the reduction of the envirnomental impact of EU consumption: Overall envirnomental impact (resource) indicators,” JRC SCIENCE AND POLICY REPORTS.

Attachment 1

INPUT				
Flow	**Category**	**Sub-category**	**Unit**	**Result**
hard coal	Resources from ground	Non-renewable energy resources from ground	MJ	3.897794274
inert rock	Resources from ground	Non-renewable material resources from ground	kg	3.868893108
Water (rain water)	Resources from water	Renewable material resources from water	kg	2.750828728
Air	Resource	in air	kg	2.541914919
natural gas	Resources from ground	Non-renewable energy resources from ground	MJ	2.134178495
crude oil	Resources from ground	Non-renewable energy resources from ground	MJ	1.548944603
sea water	Resources from water	Renewable material resources from water	kg	1.475654666
primary energy from hydro power	Resources from water	Renewable energy resources from water	MJ	0.74854656
primary energy from solar energy	Resources from air	Renewable energy resources from air	MJ	0.295311284
Uranium	Resource	in ground	MJ	0.271170285
brown coal	Resources from ground	Non-renewable energy resources from ground	MJ	0.243691462
primary energy from geothermics	Resources from ground	Renewable energy resources from ground	MJ	0.239152788
Iron	Resource	in ground	kg	0.114896977
primary energy from wind power	Resources from air	Renewable energy resources from air	MJ	0.112352191
Silicon	Resource	in ground	kg	0.076200584
Magnesium	Resource	in ground	kg	0.069011849
Aluminium ingot	Materials production	Metals and semimetals	kg	0.042670819
calcium carbonate	Resources from ground	Non-renewable material resources from ground	kg	0.027554808
carbon dioxide (biogenic)	Resources from air	Renewable material resources from air	kg	0.023377874
Chromium	Resource	in ground	kg	0.021811092
quartz sand	Resources from ground	Non-renewable material resources from ground	kg	0.017344015
clay	Resources from ground	Non-renewable material resources from ground	kg	0.013724383
Soil	Resource	in ground	kg	0.013520453
Copper	Resource	in ground	kg	0.011830143
Nickel	Resource	in ground	kg	0.010000107
river water	Resources from water	Renewable material resources from water	m3	0.007790068
from forest, used	Land use	Land transformation	m2	0.007415612
forest, used	Land use	Land occupation	m2*a	0.007414751

to forest, used	Land use	Land transformation	m2	0.00739 8509
Water to turbine - IT	Resources from water	Renewable material resources from water	m3	0.00459 3215
Oil sand (10% bitumen)	Resources from ground	Non-renewable energy resources from ground	MJ	0.00381 3479
Oil sand (100% bitumen)	Resources from ground	Non-renewable energy resources from ground	MJ	0.00332 9357
ground water	Resources from water	Renewable material resources from water	m3	0.00327 0617
from arable, irrigated, intensive	Land use	Land transformation	m2	0.00272 2136
to arable, irrigated, intensive	Land use	Land transformation	m2	0.00272 2051
sodium chloride	Resources from ground	Non-renewable material resources from ground	kg	0.00228 9787
Water to turbine	Resources from water	Renewable material resources from water	m3	0.00203 7448
biomass	Resources from biosphere	Renewable energy resources from biosphere	MJ	0.00183 4128
gravel	Resources from ground	Non-renewable material resources from ground	kg	0.00176 8499
Manganese	Resource	in ground	kg	0.00150 8362
from permanent crops	Land use	Land transformation	m2	0.00133 2614
permanent crops	Land use	Land occupation	m2 *a	0.00133 2521
to permanent crops	Land use	Land transformation	m2	0.00133 2513
natural pumice	Resource	in ground	kg	0.00130 7601
dolomite	Resources from ground	Non-renewable material resources from ground	kg	0.00129 7138
river water - DE	Resources from water	Renewable material resources from water	m3	0.00108 1871
to arable, non-irrigated, intensive	Land use	Land transformation	m2	0.00106 5112
Energy, solar, converted	Resources from air	Renewable energy resources from air	MJ	0.00103 2929
Copper scrap (>95% Cu content)	End-of-life treatment		kg	0.00101 6319
arable, non-irrigated, intensive	Land use	Land occupation	m2 *a	0.00100 6015
from arable, non-irrigated, intensive	Land use	Land transformation	m2	0.0009 88149
lake water	Resources from water	Renewable material resources from water	m3	0.0006 60455
Energy, gross calorific value, in biomass, primary forest	Resources from biosphere	Renewable energy resources from biosphere	MJ	0.00057 1979
peat	Resources from ground	Non-renewable energy resources from ground	MJ	0.00054 288
Copper cathode (>99.99 Cu)	Materials production	Metals and semimetals	kg	0.0005 00575
Energy, kinetic (in wind), converted	Resources from air	Renewable energy resources from air	MJ	0.0004 98415
oxygen	Resources from air	Renewable element resources from air	kg	0.00047 1801
bauxite	Resources from ground	Non-renewable material resources from ground	kg	0.00041 9844
Molybdenum	Resource	in ground	kg	0.00037 6131
mineral extraction site	Land use	Land occupation	m2 *a	0.00025 9154
industrial area	Land use	Land occupation	m2 *a	0.00025 0912

to unspecified, natural	Land use	Land transformation	m2	0.00022 4387
freshwater	Resources from water	Renewable material resources from water	m3	0.00019 0997
arable	Land use	Land occupation	m2 *a	0.00016 1415
from arable	Land use	Land transformation	m2	0.00013 7712
Steel scrap (St)	End-of-life treatment		kg	0.00012 3847
Transformation, from forest, natural	Resource	land	m2	0.00010 0098
bentonite	Resources from ground	Non-renewable material resources from ground	kg	9.59899 E-05
Zinc	Resource	in ground	kg	9.52336 E-05
Aggregate, natural	Resource	in ground	kg	9.14032 E-05
Pit Methane	Resources from ground	Non-renewable energy resources from ground	MJ	7.64433 E-05
stone	Resources from ground	Non-renewable material resources from ground	kg	6.91477 E-05
forest, intensive	Land use	Land occupation	m2 *a	6.65835 E-05
from shrub land	Land use	Land transformation	m2	6.45595 E-05
potassium	Resources from ground	Non-renewable element resources from ground	kg	5.48488 E-05
to arable	Land use	Land transformation	m2	5.17491 E-05
from grassland/pasture/meadow	Land use	Land transformation	m2	5.13316 E-05
Carbon, organic, in soil or biomass stock	Resources from ground	Non-renewable element resources from ground	kg	3.45948 E-05
Magnesium chloride	Resource	in ground	kg	3.19957 E-05
Titanium	Resource	in ground	kg	3.01758 E-05
to shrub land	Land use	Land transformation	m2	2.99738 E-05
Water to Cooling	Resources from water	Renewable material resources from water	m3	2.76366 E-05
dinitrogen	Resources from air	Renewable element resources from air	kg	2.50209 E-05
Lead	Resource	in ground	kg	2.03988 E-05
Magnesite	Resource	in ground	kg	1.82904 E-05
to forest	Land use	Land transformation	m2	1.78736 E-05
colemanite	Resources from ground	Non-renewable material resources from ground	kg	1.76693 E-05
from unspecified, natural	Land use	Land transformation	m2	1.61678 E-05
Phosphorus	Resource	in ground	kg	1.6081E -05
wood	Resources from biosphere	Renewable energy resources from biosphere	MJ	1.57447 E-05
from forest, primary	Land use	Land transformation	m2	1.19073 E-05
Sulfur	Resource	in ground	kg	1.14525 E-05
Fluorspar	Resource	in ground	kg	1.03071 E-05
water	Resources from water	Renewable material resources from water	m3	8.83724 E-06

arable, irrigated	Land use	Land occupation	m2 *a	7.55085 E-06
zirconium	Resources from ground	Non-renewable element resources from ground	kg	5.83497 E-06
from unspecified	Land use	Land transformation	m2	5.09621 E-06
to industrial area	Land use	Land transformation	m2	5.01917 E-06
shale	Resources from ground	Non-renewable material resources from ground	kg	3.72161 E-06

Table 12 – Inputs obtained from inventory analysis and referred to the FU – first 100 components

Attachment 2

EMISSIONS - OUTPUTS				
Flow	**Category**	**Sub-category**	**Unit**	**Result**
Water vapour	Emission to air	unspecified	kg	5.511562046
Water (evapotranspiration)	Emissions to air	Emissions to air, unspecified	kg	2.978169948
Overburden (deposited)	Deposited goods	Stockpile goods	kg	2.595912983
waste heat	Emissions to air	Emissions to air, unspecified	MJ	2.053772807
Air, used	Emission to air	unspecified	kg	1.977838793
Tailings (deposited)	End-of-life treatment	Other end-of-life services	kg	1.343569989
krypton-85	Emissions to air	Emissions to air, unspecified	kBq	0.839201358
waste heat	Emissions to water	Emissions to fresh water	MJ	0.801410609
carbon dioxide (fossil)	Emissions to air	Emissions to air, unspecified	kg	0.650723967
radon-222	Emissions to air	Emissions to air, unspecified	kBq	0.387712748
Waste (deposited)	Wastes	Other waste	kg	0.330072571
Water (rain water)	Emissions to water	Emissions to fresh water	kg	0.247810705
hydrogen-3	Emissions to water	Emissions to sea water	kBq	0.231795623
hydrogen-3	Emissions to water	Emissions to fresh water	kBq	0.080452838
Steel_EoL	End-of-life treatment	Other end-of-life services	kg	0.0653595
waste heat	Emissions to water	Emissions to sea water	MJ	0.061400356
carbon dioxide (biogenic)	Emissions to air	Emissions to air, unspecified	kg	0.022364009
xenon-135	Emissions to air	Emissions to air, unspecified	kBq	0.010193766
radium-226	Emissions to water	Emissions to fresh water	kBq	0.007335022
xenon-133	Emissions to air	Emissions to air, unspecified	kBq	0.007087368
Spoil (deposited)	Wastes	Other waste	kg	0.006919216
chloride	Emissions to water	Emissions to fresh water	kg	0.005982569
Water from turbine - IT	Emissions to water	Emissions to fresh water	m3	0.004587374
Oxygen	Emission to air	unspecified	kg	0.003947953
hydrogen-3	Emissions to air	Emissions to air, unspecified	kBq	0.003493934

sulfur dioxide	Emissions to air	Emissions to air, unspecified	kg	0.00309884
overburden (unspecified)	Wastes	Mining waste	kg	0.001892187
xenon-138	Emissions to air	Emissions to air, unspecified	kBq	0.001758771
xenon-137	Emissions to air	Emissions to air, unspecified	kBq	0.001601895
Copper_EoL	End-of-life treatment	Other end-of-life services	kg	0.001464053
Water	Emissions to water	Emissions to sea water	m3	0.001452889
nitrogen dioxide	Emissions to air	Emissions to air, unspecified	kg	0.001445316
carbon monoxide (fossil)	Emissions to air	Emissions to air, unspecified	kg	0.001258742
Clean gas	Emissions to air	Emissions to air, unspecified	kg	0.001240515
stainless steel scrap (430, from external supply)	Wastes	Production residues	kg	0.001118955
methane (fossil)	Emissions to air	Emissions to air, unspecified	kg	0.001107331
carbon-14	Emissions to air	Emissions to air, unspecified	kBq	0.001104426
particles (> PM10)	Emissions to water	Emissions to fresh water	kg	0.001102433
chloride	Emissions to water	Emissions to sea water	kg	0.001061815
Carbon dioxide (land use change)	Emissions to air	Emissions to air, unspecified	kg	0.000653694
argon-41	Emissions to air	Emissions to air, unspecified	kBq	0.000608095
particles (> PM10)	Emissions to air	Emissions to air, unspecified	kg	0.000498602
xenon-131	Emissions to air	Emissions to air, unspecified	kBq	0.000381876
sulfate	Emissions to water	Emissions to fresh water	kg	0.000343507
chemical oxygen demand	Emissions to water	Emissions to fresh water	kg	0.00030394
particles (PM2.5)	Emissions to air	Emissions to air, unspecified	kg	0.000233876
sodium	Emissions to water	Emissions to fresh water	kg	0.000206859
iron	Emissions to water	Emissions to fresh water	kg	0.000195945
calcium	Emissions to water	Emissions to fresh water	kg	0.000191092
carbon-14	Emissions to water	Emissions to sea water	kBq	0.00017643
thorium-230	Emissions to water	Emissions to fresh water	kBq	0.000166352
carbon dioxide (biogenic)	Emissions to air	Emissions to non-urban air or from high stacks	kg	0.000154657
Used hot water tank			Item(s)	0.000130719
particles (PM2.5 - PM10)	Emissions to air	Emissions to air, unspecified	kg	0.000127308
waste heat	Emissions to air	Emissions to urban air close to ground	MJ	0.000105899
Radioactive tailings	Wastes	Radioactive waste	kg	0.000103265
ruthenium-106	Emissions to water	Emissions to sea water	kBq	9.53673E-05
hydrogen sulfide	Emissions to air	Emissions to air, unspecified	kg	8.68408E-05
nitrate	Emissions to water	Emissions to fresh water	kg	8.616E-05

total organic carbon	Emissions to water	Emissions to fresh water	kg	8.57344E-05
uranium-238	Emissions to water	Emissions to fresh water	kBq	8.48056E-05
dinitrogen	Emissions to air	Emissions to air, unspecified	kg	8.33278E-05
uranium-234	Emissions to water	Emissions to fresh water	kBq	6.50485E-05
non-methane volatile organic compounds	Emissions to air	Emissions to air, unspecified	kg	6.32136E-05
Nitrogen monoxide	Emission to air	unspecified	kg	5.66354E-05
carbonate	Emissions to water	Emissions to fresh water	kg	5.5378E-05
sulfate	Emissions to water	Emissions to water, unspecified (long-term)	kg	5.10337E-05
fluoride	Emissions to water	Emissions to fresh water	kg	5.08932E-05
sodium	Emissions to water	Emissions to water, unspecified (long-term)	kg	5.05311E-05
carbon dioxide (fossil)	Emissions to air	Emissions to urban air close to ground	kg	4.75942E-05
nickel	Emissions to air	Emissions to air, unspecified	kg	4.42963E-05
hydrogen chloride	Emissions to air	Emissions to air, unspecified	kg	4.16957E-05
Water from cooling - IT	Emissions to water	Emissions to fresh water	m3	4.02831E-05
carbon dioxide (biogenic)	Emissions to air	Emissions to urban air close to ground	kg	3.76033E-05
uranium-238	Emissions to air	Emissions to air, unspecified	kBq	3.52E-05
calcium	Emissions to water	Emissions to water, unspecified (long-term)	kg	3.24781E-05
iodine-131	Emissions to water	Emissions to sea water	kBq	3.09944E-05
carbon dioxide (fossil)	Emissions to air	Emissions to non-urban air or from high stacks	kg	3.055E-05
Particulates, > 10 um	Emission to water	ocean	kg	2.9278E-05
cesium-137	Emissions to water	Emissions to sea water	kBq	2.83453E-05
Water	Emissions to water	Emissions to water, unspecified	m3	2.60912E-05
Solids, inorganic	Emissions to water	Emissions to fresh water	kg	2.3178E-05
propane	Emissions to air	Emissions to air, unspecified	kg	2.31415E-05
ethane	Emissions to air	Emissions to air, unspecified	kg	1.9635E-05
biological oxygen demand	Emissions to water	Emissions to fresh water	kg	1.9568E-05
carbonate	Emissions to water	Emissions to sea water	kg	1.91159E-05
Water	Emissions to air	Emissions to air, unspecified	m3	1.70071E-05
Glass wool	Wastes	Radioactive waste	kg	1.59477E-05
iodine-131	Emissions to air	Emissions to air, unspecified	kBq	1.49886E-05
sulfate	Emissions to water	Emissions to water, unspecified	kg	1.33002E-05
Particulates, < 10 um	Emission to air	unspecified	kg	1.20571E-05
cesium-137	Emissions to water	Emissions to fresh water	kBq	1.1151E-05
nitrous oxide	Emissions to air	Emissions to air, unspecified	kg	1.09236E-05

Ammonium, ion	Emission to air	unspecified	kg	1.02695E-05
hydrogen	Emissions to air	Emissions to air, unspecified	kg	1.02332E-05
sulfide	Emissions to water	Emissions to fresh water	kg	1.00384E-05
Oils, unspecified	Emissions to water	Emissions to fresh water	kg	9.74954E-06
magnesium	Emissions to water	Emissions to fresh water	kg	9.48299E-06
methane (biogenic)	Emissions to air	Emissions to air, unspecified	kg	9.43827E-06
Nitrogen oxides	Emissions to air	Emissions to air, unspecified	kg	8.97351E-06

Table 13 – Emissions obtained from inventory analysis and referred to the FU – first 100 components